# Chapter V

# CONVERSION TO PHYSICAL QUANTITIES


| | |
|---|---|
| **DOI** | https://doi.org/10.25935/vps6-jb33 |
| **Publisher** | MASER/PADC |
| **Citation** | Sitruk, L. & Manning, R. (**2022**) *The GGS/WIND/Waves Experiment* – Chapter 5 (Version 4.3, translated by A. Fave). MASER/PADC. doi:10.25935/VPS6-JB33 |
| **License** | CC-BY-4.0 |



**Summary**

The purpose of instrumental calibrations is to bring the raw telemetry data back to the physical values at the input of the antennas. A distinction is made between pre-launch ground calibrations, which determine the response of the receivers in different configurations, and in-flight or internal post-launch calibrations, which are intended to test possible drifts in the instrumental responses. In this chapter, we describe the ground test equipment as well as the white noise generator (generator of pseudo-random binary sequences). For the RAD1/2 receivers, we measure essentially the response in gain (AGC) and in frequency in various configurations. We also measure the R ratio, useful for determining the characteristics of the sources. For the TNR instrument, we measure the gain response (AGC value and frequency channel outputs) in different configurations. The response curve of the AGC circuit is modeled by a law called "logarithmic law". We deduce by numerical adjustment to this theoretical model four calibration parameters. The sequence of the internal calibration orders of the experiment is given. The current state of the calibration analysis is presented.

## Content

5. Conversion in Physical Quantities ........................................................................................................179
5.1. General........................................................................................................................................179
5.1.1. Principle of calibrations ...........................................................................................................179
5.1.2. Ground calibrations .................................................................................................................180
5.2. Ground calibration equipment ...................................................................................................181
5.3. The different tests.......................................................................................................................185
5.4. Characteristics of the noise generator .......................................................................................185
5.5. Ground calibration tests .............................................................................................................190
5-5-1 Frequency response of RAD1/2 receivers: tests 10 and 20 .....................................................190
5-5-2 Amplitude response of RAD1/2 receivers: tests 11 and 21 .....................................................192
5.5.3. Measuring the R-ratio: tests 12 and 22 ...................................................................................194
5.5.4. TNR receiver response to white noise: digital spectrum (test 30) ..........................................203
5-5-5. TNR receiver amplitude response: test 31................................................................................207
5-5-6 Physical magnitude of a TNR digital spectrum .........................................................................208
5.6. Digital adjustment of the amplitude response of the receivers .................................................213
5.6.1. Modeling of the receivers response .........................................................................................213
5.6.2. Formulas of deriving physical quantities of the AGC ...............................................................215
5.7. Internal calibration (test 4)..........................................................................................................216
5.7.1. General ....................................................................................................................................216
5.7.2. Configurations considered .......................................................................................................219
5.8. Evaluation of the calibration tests .............................................................................................224
5.8.1. TNR calibrations .......................................................................................................................224
5-8-2 RAD1/2 Calibrations .................................................................................................................228

# 5. Conversion in Physical Quantities

## 5.1. General

### 5.1.1. Principle of calibrations

Throughout the mission, the WIND satellite transmits a stream of binary telemetry data to the ground. The use of this data for scientific analysis requires the ability to trace the raw data to the physical quantities in the ambient plasma at the antenna input.

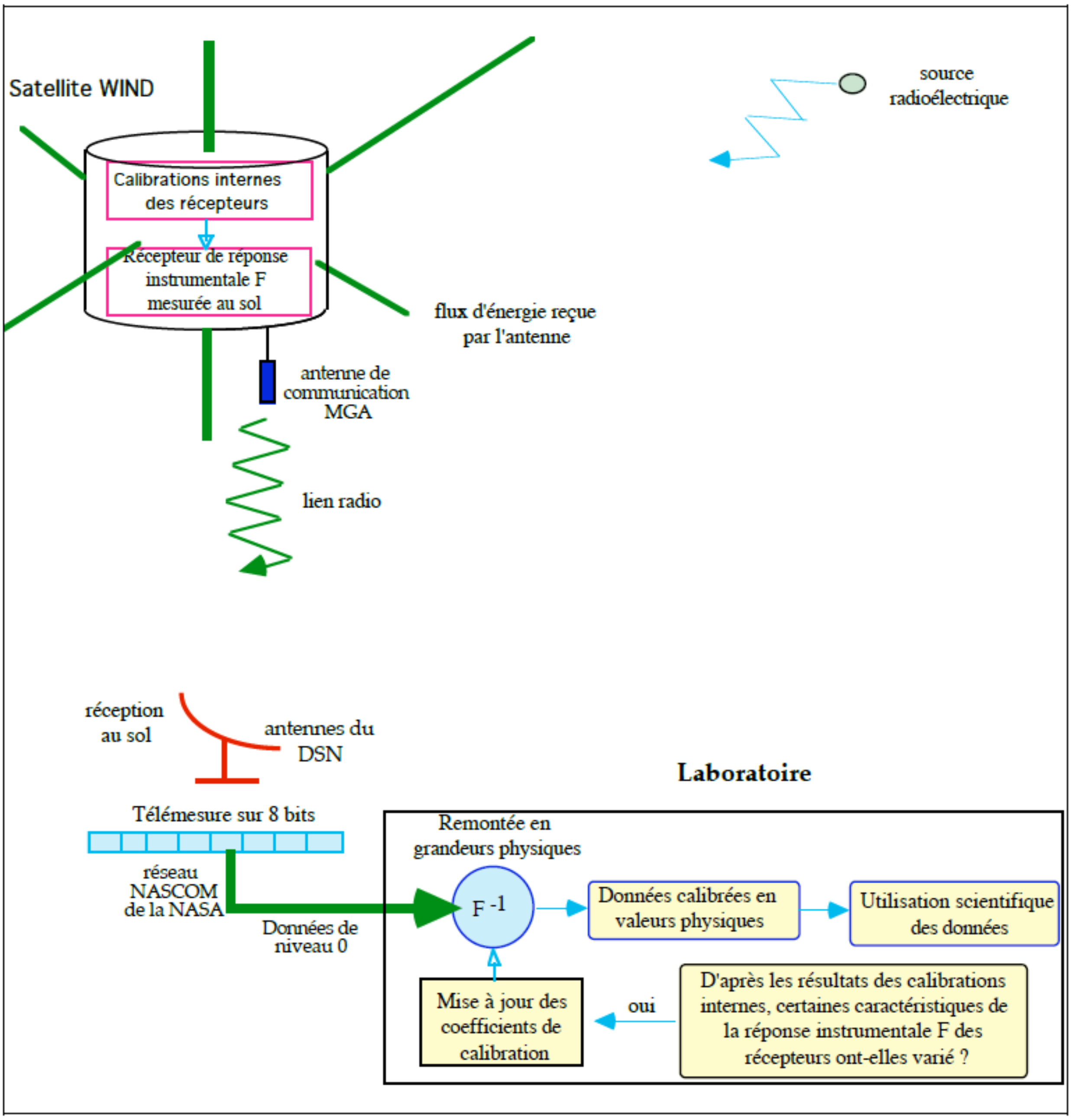


Fig. Principle of routine calibration processing

To do this, the response characteristics of the on-board receivers[1], subjected to various stresses (different input signal levels, different reception frequencies, different temperatures, ...) are studied on the ground on the flight model, before the launch. Such measurements are called ground calibrations. They constitute the reference baseline of the instrumental responses before launch. In practice, these measurements result in the constitution of a file of calibration coefficients[2], used routinely for the physical size of the raw telemetry data.

These ground measurements are however insufficient. Indeed, the characteristics of the receivers are likely to evolve during the mission because of the environment, the ageing of the electronic components, the ambient temperature, possible impacts of cosmic particles, etc.... This is why the same type of measurements are also carried out during the mission: these are the in-flight or "internal" calibrations. Calibration sequences are then periodically applied to the receivers by means of a noise generator internal to the experiment. These sequences are a condensation of the multiple ground calibration tests. The internal calibration measurements are also transmitted to the telemetry. By comparison with the reference baseline of the calibration measurements made on the ground, it is possible to detect a possible drift of the response of the receivers. The receiver calibration coefficients file is then updated. These are not called into question if it turns out that only the internal noise generator has changed. (AC) Let us specify that unlike other types of on-board experiments, the transfer functions of the "wave" receivers evolve relatively little during the operational life of the satellites.

The quality of the calibration measurements, especially those carried out before launch, conditions the quality of the experiment as a whole and the accuracy of the physical data obtained. They allow to estimate precisely the signal level and to subtract the background noise from the data. The TNR instrument, which collects a low intensity noise, is particularly sensitive to the accuracy of these calculations.

The programs for physical quantities developed by M. Reiner, C. Meetre and K. Goetz can be found in the directory: WIND_PHYSICAL.

### 5.1.2. Ground calibrations

The Noise Generator (GB or NG) is a standard noise source used for ground calibrations. It is a generator of pseudo-random binary sequences, manufactured at DESPA. It provides a white noise in a certain frequency range. In this case, 7 frequency bands can be selected: they are noted A, B, C, D, E, for the five frequency bands of the TNR receiver, HF1 for the RAD1 receiver, and HF2 for the RAD2 receiver.

1) For RAD1 and RAD2 receivers, three types of tests are performed:

- Measurement, at a fixed frequency, of the amplitude (gain) at the output of the receiver for different values of attenuation of the input signal.

- Measurement of the frequency response curve of each receiver, for a given value of the receiver's input amplitude.

Different configurations are tested:

[1] We also speak of transfer function of receivers. However, it should be noted that this designation corresponds, in signal processing, to the Fourier transform of the impulse response of a system. Here, in addition to the frequency response, we also measure the gain response due to the AGC circuit, the temperature response, etc. ....

[2] Measurements are made at particular frequencies and AGC levels, so these instrumental responses are discrete functions. Calibration coefficients must be applied to the raw telemetry values for a given frequency and AGC level, ...

| Mode | Entry on which is applied the signal | Reading the output signal |
|---|---|---|
| Sep | X or Y and Z | in S and Z channels |
| Sum | X or Y and Z | in S/S' and Z channels |
| Sum | Z only | in S/S' channel |
| Sep | Z only | in channel S: crosstalk measurement |
| Sep | X or Y only | in channel Z: crosstalk measurement[3] |

- phase measurements.

2) The TNR receiver is calibrated as follows:

- Measurement, at a fixed frequency, of the amplitude (gain) at the output of the receiver for different values of attenuation of the input signal.

- Measurement of the frequency response curve of each receiver, for a given value of the receiver's input amplitude.

The particularity of the TNR receiver is that it gives both an AGC value and a digital spectrum at the output. These two components of the output signal must therefore be calibrated.

3) The noise voltage of the GB without attenuation is also calibrated (" 0dB " ).

Calibrations in "hybrid" mode and crosstalk measurement

“Hybrid" calibration consists, in SUM mode, in reading the output signal of channel S, after having applied a signal to the input of channel Z only, or in reading the output signal of channel Z, after having applied a signal to the input of channel X (or Y) only.

In theory, when we are in a SEP configuration, and a signal is applied to channel X (resp. Z), we should not measure an output signal on channel Z (resp. S). In practice, however, we observe this phenomenon of electrical interference between the two channels: this is the phenomenon known as crosstalk.

## 5.2. Ground calibration equipment

The GB stimulates one of the inputs of the Waves experiment through an electromechanical relay (R/B) and a preamplifier. The chain of calibration equipment of the Waves experiment can be schematized as follows:

[3] Inverse case of the previous one.

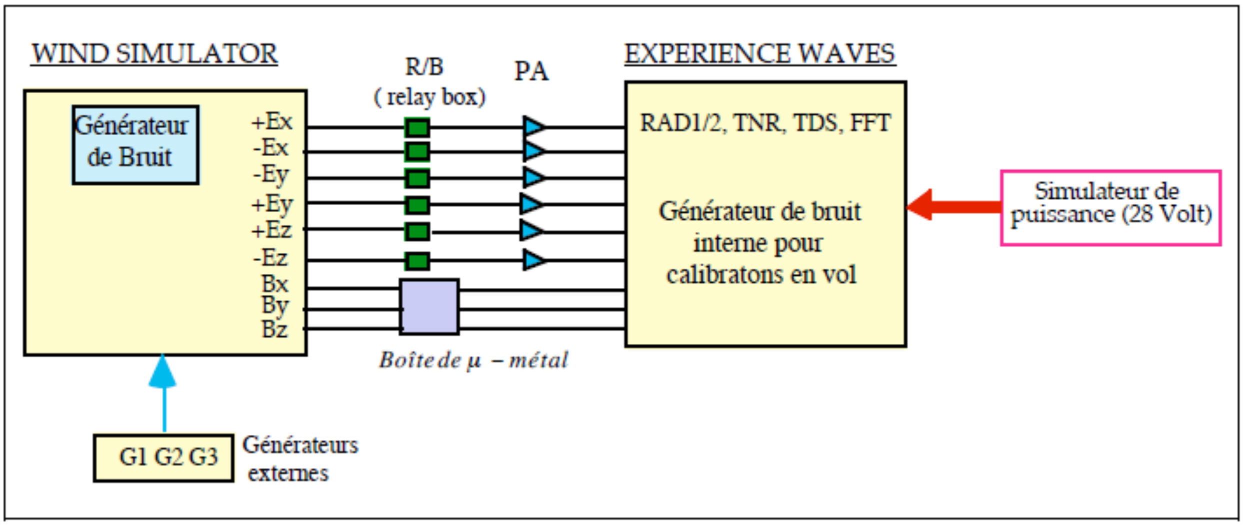


Fig. Synoptic diagram of the calibration equipment

In the "WIND simulator" you have the following possibilities:

- use the external generators[4] of frequency G1, G2 (G3 is used for Waves 2) or a new generator (see phase tests).

- use the GB, for which we have 7 possible frequency bands, corresponding to the 7 following switches: A, B, C, D, E for the 5 TNR bands, HF1 for RAD1, and HF2 for RAD2.

The "WIND Simulator" in the above diagram can be detailed as follows (based on a more general diagram by G. NICOL):

[4] G1, G2, G3 are identical in design.

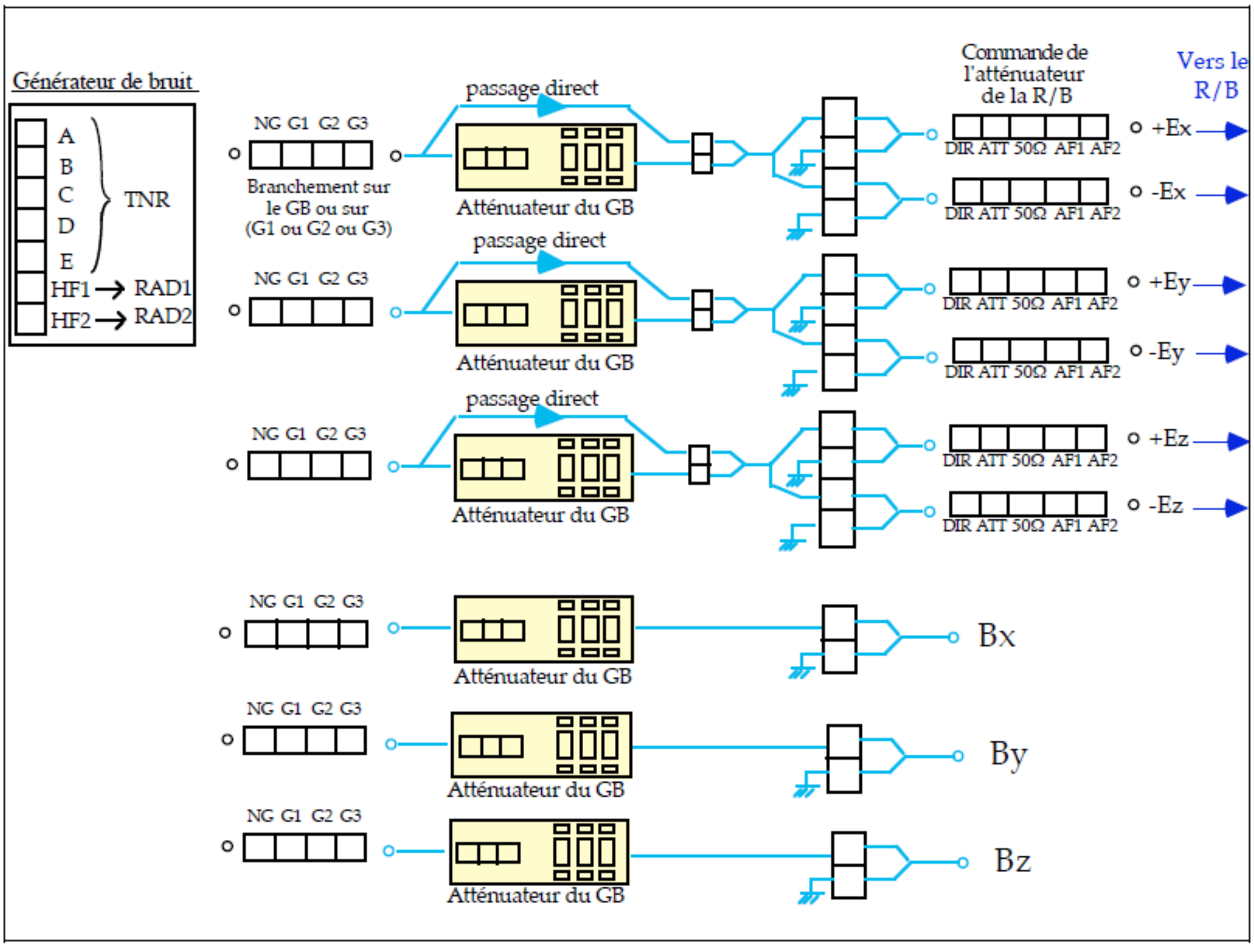


Fig. Front panel of the "WIND SIMULATOR" (simplified diagram)

The attenuation levels of the GB range from 0 to 126 dB. Be careful to distinguish between the attenuation levels of the GB (0 to 126 dB, in 2 dB steps), and the 5 attenuation possibilities of the variable R/B attenuator.

Variable R/B attenuator

The diagram above shows that the GB can be connected to the electromechanical relays, either by passing through the variable attenuator or by short-circuiting it (direct passage).

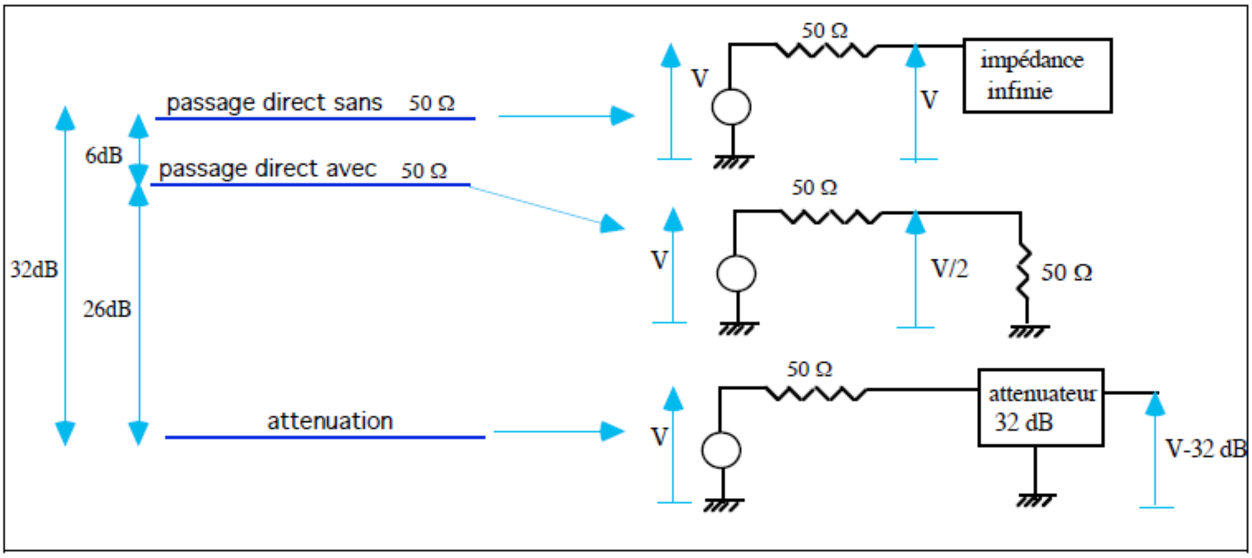


Fig. Different attenuation possibilities

• On the top electronic diagram, there is no attenuation. The impedance being infinite, we find the voltage V. On the bottom electronic diagram, the attenuation is 32 dB. On the middle electronic diagram, we find a voltage of middle, we find a voltage of V/2, that is to say an attenuation of 6 dB:

$$20 \log\left(\frac{V/2}{V}\right) = -6\ dB\ .$$

The attenuation is therefore:

- 0 dB. This corresponds to the DIR push-button (fig. ).

- 32 dB compared to the direct passage without (infinite 50 Ω impedance). This corresponds to the ATT push-button (fig. ).

- 26 dB in relation to the direct pass with 50 Ω: in the case of direct pass, we can close on 50 Ω which attenuates the signal by dB6. With an attenuation of dB26, the attenuation levels of the GB are shifted from the range [0 dB, 126 dB] to the range [26 dB, 126 + 26 dB]. This corresponds to the push button 50 Ω (or ATT and 50 Ω).

- There are also the following possibilities: dummy antenna 1, dummy antenna 2, (?) . This corresponds to push buttons AF1 and AF2.

• In general, it is preferred to use the attenuator to obtain better noise protection. For the HF2 range, the electrical energy per unit of frequency transmitted by the GB is lower because the energy is spread over a wide range of frequencies; therefore, a stronger signal must be applied and no attenuation is used.

• It is also possible to connect to ground or to activate (+ or - $E_x$) or (+ or - $E_y$), or (+ or - $E_z$).

• The equipment can be controlled in "local" mode (i.e. manually, using the switches on the front panel of the instrument) or in "remote" mode (by software).

## 5.3. The different tests

A program written in script language, written by the University of Minnesota team, sends commands to the ground test equipment. The calibration tests are numbered. We have the following[5] tests:

| Test number | Nature of the test |
|---|---|
| 4 | Internal calibration test |
| 10 | Frequency response of RAD1 |
| 11 | Amplitude response of RAD1 (log law) |
| 12 | Response in ARD phase1 |
| 20 | Frequency response of RAD2 |
| 21 | Amplitude response of RAD2 (log law) |
| 22 | Response in ARD2 phase |
| 30 | Frequency response of TNR |
| 31 | Amplitude response of TNR (log law) |
| 40 and following | FFT calibrations |
| 50 and following | TDS calibrations |

This numbering system is derived from the ULYSSES/URAP receiver calibrations.

Only one temperature, 20°, is considered. In principle, in flight, the temperature is very close to the nominal temperature, itself very close to the ambient temperature. Several tests of temperature variation were carried out on the identification model.

The document "Calibration Documentation" [SIT93] gives details of the operations actually carried out during the tests 10,11, 20, 21, 30, 31.

For the tests 10, 11, 12, 20, 21, 22, please refer to the general diagram of the RAD1/2 receivers.

For ground calibrations, a dipole configuration is not possible because of the presence of baluns between the antenna and the PA: the signal is applied either to the $+E_x$ channel, connecting $-E_x$ to ground, or to the $-E_x$ channel, connecting $+E_x$ to ground, similarly for the $E_y$ and $E_z$ channels.

## 5.4. Characteristics of the noise generator

The noise generator (GB) is internal to the "WIND generator". It is manufactured at DESPA [BOU79]. It is a generator of pseudo-random binary sequences (stable pulses, constant amplitude), made from digital circuits [MAX]. The amplitude of the binary sequences of the GB is 5V peak to peak and the maximum voltage of this signal Vmax is half of the amplitude of the square wave signal, that is to say here 2.5 Volts.

[5] The test numbers with tens of a digit greater than 3 are for Waves2

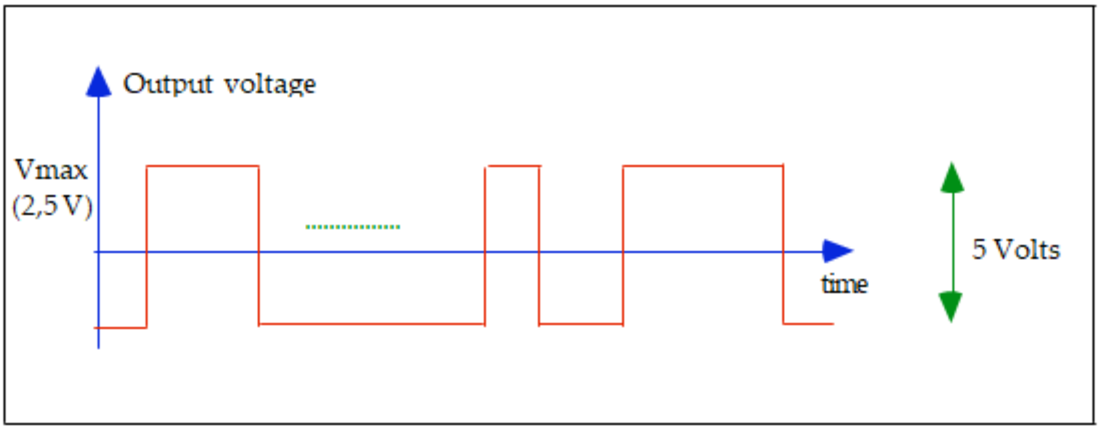


Fig. Pseudo-random binary sequences

An internal clock clocked at a certain frequency controls the sequencing of this circuit. The principle diagram of a pseudo-random binary sequence generator is as follows:

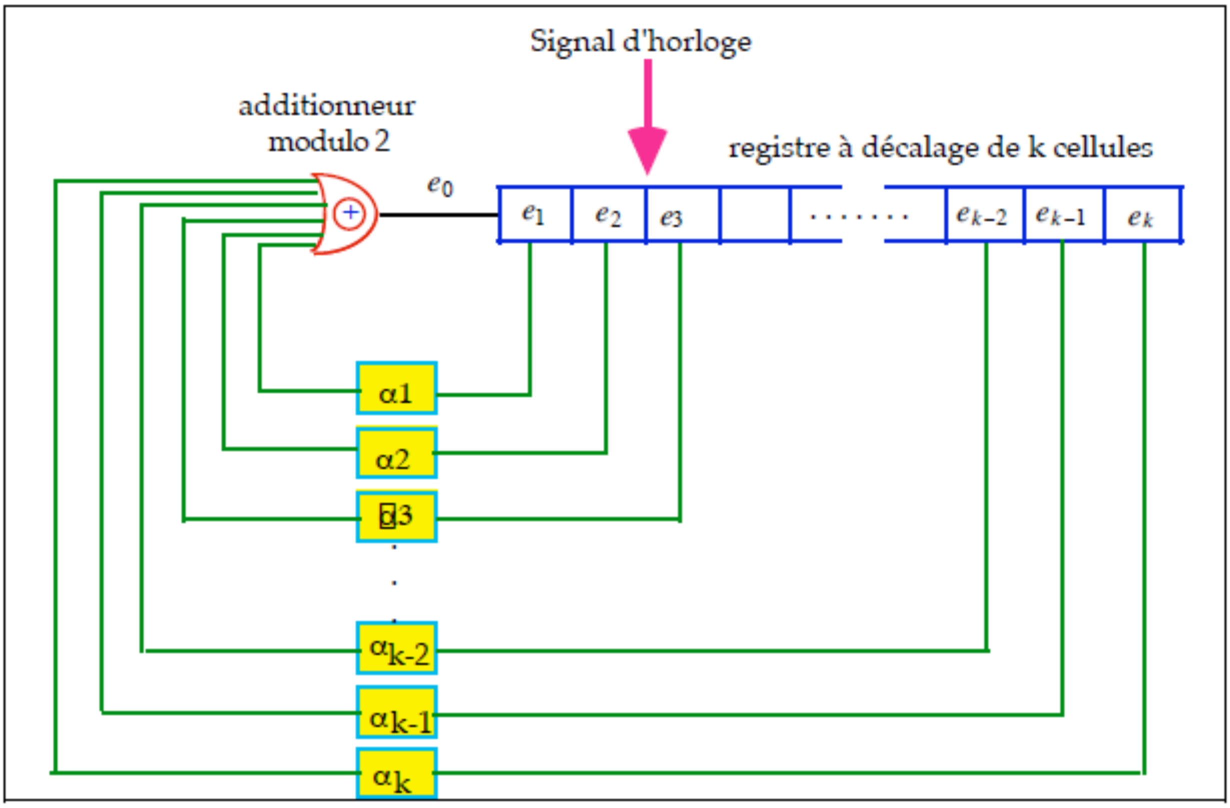


Fig. Schematic diagram of a pseudo-random noise generator

It is a shift register with serial input and parallel output which has as input a suitable combination of the contents of each of the cells. The input circuit generating $e_0$ is an adder modulo 2, the quantities $\alpha_1$, $\alpha_2$, ..., $\alpha_k$ are multiplier coefficients by 0 or 1.

It is shown that in the case of such a circuit, the power spectral density $F(f)$ of the signal is approximately in the form of a cardinal sine, with a first minimum for $f = F_{horloge} = 1/\theta$ :

$$F(f) = V_{max} \cdot \left( \frac{\sin \pi f \theta}{\pi f} \right)$$

with 1/θ : clock frequency of the digital circuit.

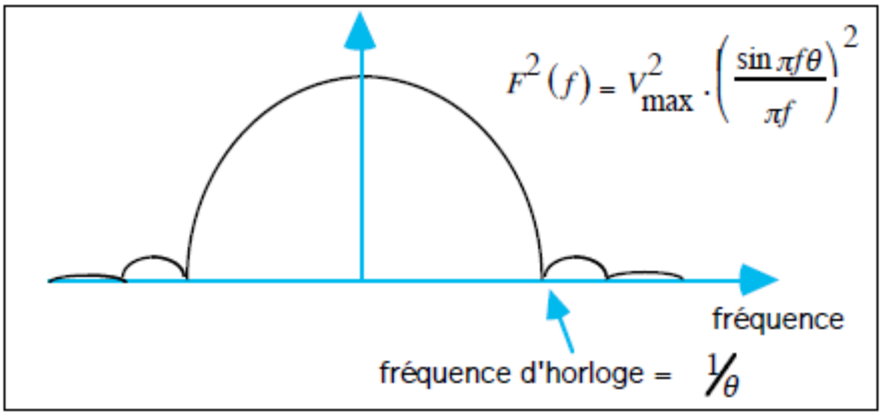


According to the energy properties of signals, formulated by Parseval's theorem, the energy contained in a signal is identical to the energy contained in its spectrum. The latter is here the energy of a rectangular signal between – θ/2 and θ/2. We deduce (calculation TBC):

$$Energie = \int_{-\infty}^{+\infty} V_{max}^2 \left( \frac{\sin \pi f \theta}{\pi f} \right)^2 df = \frac{V_{max}^2 \cdot \theta}{2} = \frac{V_{max}^2}{2 \cdot F_{horloge}}$$

We check that we have the unit of *Volts²/Hertz*.

For the various calibrations, we need to know the "0 dB" of the GB, which corresponds to the noise voltage without attenuation. The RMS voltage of noise without attenuation is written, if we extract the square root of the result and divided by √2 to obtain effective volts:

$$\boxed{V_0 = \frac{V_{max}}{2 \cdot \sqrt{F_{horloge}}}}$$

We have then as unit *Volts* / √*Hertz*

We can measure $V_0$ using a spectrum analyzer and summing the contributions of the different lines.
For the different clock frequencies, we have ($dB_0$ is measured by reference to 1 $\mu V/\sqrt{Hz}$):

| Frequencies band of GB | Clock frequency of GB | $V_0$ (noise voltage) without attenuation | $dB_0=20\log_{10}(V_0)$ |
|---|---|---|---|
| A | 78.125 kHz | 4472 $\mu V/\sqrt{Hz}$ | -47 dB |
| B | 156.25 kHz | 3162 $\mu V/\sqrt{Hz}$ | -50 dB |
| C | 312.5 kHz | 2236 $\mu V/\sqrt{Hz}$ | -53 dB |
| D | 625 kHz | 1581 $\mu V/\sqrt{Hz}$ | -56 dB |
| E | 1.25 MHz | 1118 $\mu V/\sqrt{Hz}$ | -59 dB |
| HF1 | 5 MHz | 559 $\mu V/\sqrt{Hz}$ | -65 dB |
| HF2 | 40 MHz | 198 $\mu V/\sqrt{Hz}$ | -74.1 dB |

As one can see, the dB0 values evolve from 3 dB to 3 dB, when one passes from one band to the other (bands A to E). Indeed, the GB clock frequency being multiplied by 2 from one band to another, V0 is divided by $\sqrt{2}$ , hence the evolution of 3dB in 3 dB.

The quantity $V_0$ integrates all the energy of the signal distributed over all frequencies. However, the noise spectrum of the GB is not flat (cardinal sine), it is necessary to consider the notion of noise power generated as a function of frequency, which amounts to defining the function $V_0(f)$ . This variation in frequency is explained by the shape of the cardinal sine and by the electronics. However, measurements have shown that this variation is small and the difference is only 0.6 dB from one end to the other.

We systematically position ourselves in the practically flat region of the frequency spectrum (region close to the origin), as can be seen on the following diagram (example of the TNR A band):

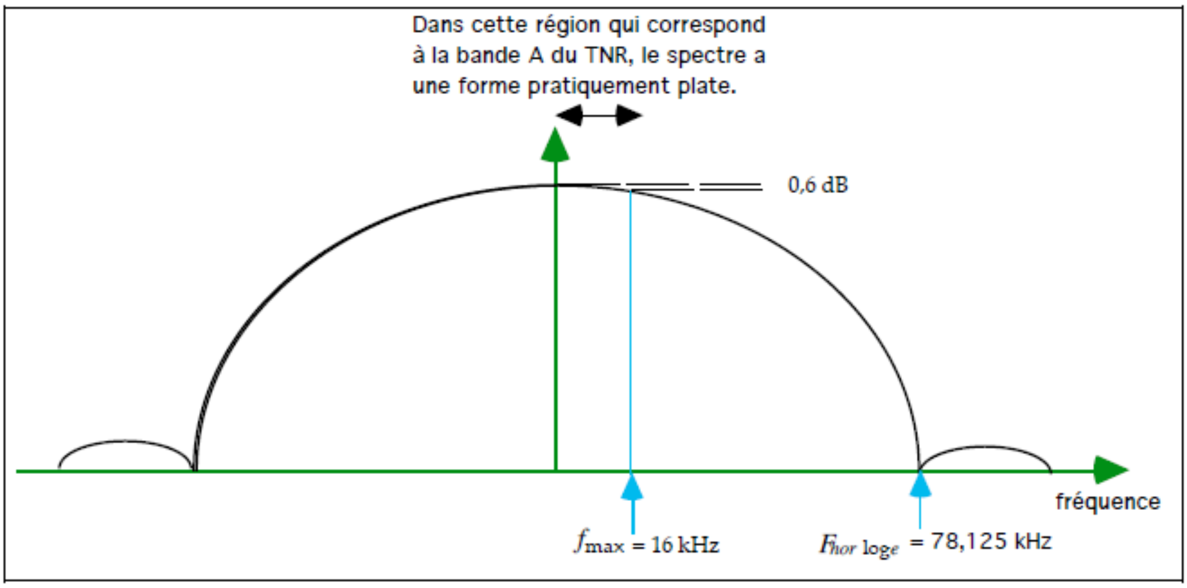

The clock frequency $F_{horloge}$ is indeed taken equal to about 5 times the maximum frequency $f_{\max}$ of the band, that is:

$$\frac{f_{\max}}{F_{horloge}} = \frac{1}{5}$$

The calculation of the attenuation is then as follows [MAX]:

$$\left(\frac{\sin(\pi f_{\max}\theta)}{\pi f_{\max}\theta}\right)^2 = \left(\sin\left(\pi\frac{f_{\max}}{F_{horloge}}\right)\Big/\left(\pi\frac{f_{\max}}{F_{horloge}}\right)\right)^2 = \left(\sin\left(\frac{\pi}{5}\right)\Big/\left(\frac{\pi}{5}\right)\right)^2 = 0,875$$

That is: $10 \log(0{,}875) = -0{,}5799 \approx -0{,}6\ dB$

This value confirms the experimental measurements.

Recently found reference values are as follows:

| Frequency band | $dB_0$ (old values) | $dB_0$ (new values) |
|---|---|---|
| A | -46.36 | -40.36 |
| B | -49.47 | -43.47 |
| C | -52.62 | -46.62 |
| D | -55.63 | -49.63 |
| E | -58.64 | -52.64 |

It can be seen that the values are very close to the values given in the previous table. It was necessary to subtract 6 *dB* recently to take into account ?... TBD

In fact, R. Manning notes that these values also depend on the downstream assembly of the GB.

The reference values for the RAD1 and RAD2 receivers were numerically adjusted as a function of frequency. We consider the following model:

$$dB_0(f) = a(0) + a(1)\cdot f + a(2)\cdot f^2 + a(3)\cdot f^3$$

where $f$ is the frequency. The polynomial coefficients obtained are the following:

| | RAD1 $E_x$ | RAD1 $E_y$ | RAD1 $E_z$ | RAD2 $E_y$ | RAD2 $E_z$ |
|---|---|---|---|---|---|
| $a(0)$ | -64.10 | -63.93 | -64.30 | -73.87 | -74.27 |
| $a(1)$ | -8.798 $10^{-3}$ | 4.53 $10^{-3}$ | 2.624 $10^{-3}$ | -9.559 $10^{-3}$ | -8.958 $10^{-3}$ |
| $a(2)$ | 5.28 $10^{-5}$ | -5.802 $10^{-5}$ | -3.470 $10^{-5}$ | -6.615 $10^{-5}$ | -5.786 $10^{-5}$ |
| $a(3)$ | -1.59 $10^{-7}$ | 1.106 $10^{-7}$ | 5.662 $10^{-8}$ | -3.623 $10^{-8}$ | -1.126 $10^{-8}$ |

We can compare these values to the values found theoretically for the HF1 and HF2 ranges. Plots TBW.

# 5.5. Ground calibration tests

## 5-5-1 Frequency response of RAD1/2 receivers: tests 10 and 20

The test 10 (respectively 20) consists in tracing the frequency response of the receiver RAD1 (respectively RAD2) for a given level of attenuation. It is thus a question of tracing a spectrum, which has the following appearance:

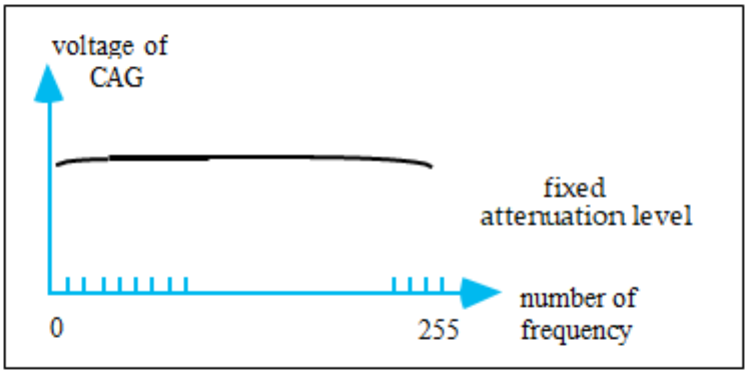


Fig. Test 10 or 20

For this test, the GB is used (frequency range HF1 for the test 10 and HF2 for the test 20), at a fixed attenuation level.

- Test 10

- The attenuation level of the GB is:

- 30 dB, for the case when connected to the $E_x$.
- 40 dB, in case of connection to the $E_y$ or $E_z$ antenna.

The difference in the attenuation values is due to the fact that the PAs do not have the same gains, since the longer $E_x$ antenna is supposed to collect a stronger signal.

-18 configurations (antennas, SUM/SEP) for one attenuation level are used:

| Step | Selection of antennas | | | configuration |
|---|---|---|---|---|
| 1 | $+E_x$ | | $+E_z$ | SEP |
| 2 | $-E_x$ | | $+E_z$ | SEP |
| 3 | | $+E_y$ | $-E_z$ | SEP |
| 4 | | $-E_y$ | $-E_z$ | SEP |
| 5 | $+E_x$ | | $+E_z$ | SUM |
| 6 | $-E_x$ | | $+E_z$ | SUM |
| 7 | $+E_x$ | | $-E_z$ | SUM |
| 8 | $-E_x$ | | $-E_z$ | SUM |
| 9 | | $+E_y$ | $+E_z$ | SUM |
| 10 | | $-E_y$ | $+E_z$ | SUM |
| 11 | | $+E_y$ | $-E_z$ | SUM |
| 12 | | $-E_y$ | $-E_z$ | SUM |
| 13 | $+E_x$ | | | SUM |
| 14 | | | $+E_z$ | SUM |
| 15 | $-E_x$ | | | SUM |
| 16 | | | $-E_z$ | SUM |
| 17 | | $+E_y$ | | SUM |
| 18 | | $-E_y$ | | SUM |

- The background noise is recorded at the end of the test 10 when the mode is SUM. To perform this measurement, the GB is switched off.

A "hybrid Z" type calibration is also being considered (SUM mode necessarily, in this case).

- <u>Test 20</u>

-Direct pass: no attenuator for the R/B.

-We use 5 levels of GB attenuation: from 0 to 80 dB, in steps of 20 dB (the test 20 is much faster than the test 10).

-The following 10 configurations (antennas, SUM/SEP mode) are used:

| Step | Antennas | | Mode |
|---|---|---|---|
| 1 | $+E_y$ | $+E_z$ | SEP |
| 2 | $-E_y$ | $-E_z$ | SEP |
| 3 | $+E_y$ | $+E_z$ | SUM |
| 4 | $-E_y$ | $+E_z$ | SUM |
| 5 | $+E_y$ | $-E_z$ | SUM |
| 6 | $-E_y$ | $-E_z$ | SUM |
| 7 | $+E_y$ | | SUM |
| 8 | | $+E_z$ | SUM |
| 9 | $-E_y$ | | SUM |
| 10 | | $-E_z$ | SUM |

These 10 steps are repeated for each of the 5 mitigation levels:

0 dB: step1, step 2,.......... step 10.
20 dB: step1, step 2,.......... step 10.
40 dB: step1, step 2,.......... step 10.
60 dB: step1, step 2,.......... step 10.
80 dB: step1, step 2,.......... step 10.

- The background noise (with GB off) is recorded at the end of the test.

### 5-5-2 Amplitude response of RAD1/2 receivers: tests 11 and 21

The test 11 (respectively 21) consists in plotting the amplitude response of the RAD1 (respectively RAD2) receiver. The calibration curve obtained has the following appearance:

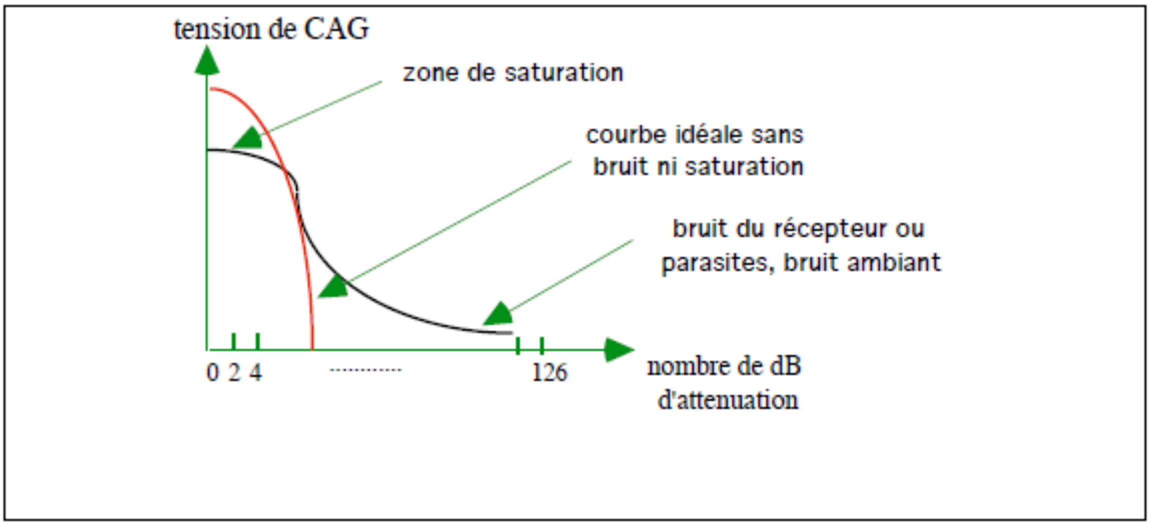


Fig. Test 11 or 21: response of the AGC circuit as a function of the input signal amplitude, at a given frequency

- These tests are all done in SEP[6] mode: the signal is applied to the Z and X channels (RAD1) and to the Z and Y channels (RAD2).

- We use the GB (frequency range HF1 for the test 11 and HF2 for the test 21), at a variable level of attenuation of the GB from 0 to 126 dB, in steps of 2 dB.

- For each curve, we position ourselves on a single frequency: "freeze" mode. We repeat this operation for 16 different frequencies in the case of RAD1 and 17 different frequencies in the case of RAD2.

[6] This test is of no interest in SUM mode, because we want to obtain a curve like the one shown. We can therefore have only one input signal.

The 16 following frequencies are used for the test 11:

| Index | 0 | 2 | 4 | 6 | 8 | 15 | 21 | 29 | 43 | 64 | 81 | 130 | 180 | 206 | 230 | 255 |
|---|---|---|---|---|---|---|---|---|---|---|---|---|---|---|---|---|
| Value (in kHz) | 20 | 28 | 36 | 44 | 52 | 80 | 104 | 136 | 192 | 276 | 344 | 540 | 740 | 844 | 940 | 1040 |

As can be seen, we choose a higher number of low frequencies where we find a greater variation. We go until to 1040 be in adequacy with range of frequencies RAD2.

For the test 21, we use 17 equally spaced frequencies (there is no obvious variation to analyze):

| Index | 0 | 16 | 32 | 48 | 64 | 80 | 96 | 112 | 128 | 144 | 160 | 176 | 192 | 208 | 224 | 240 | 255 |
|---|---|---|---|---|---|---|---|---|---|---|---|---|---|---|---|---|---|
| Value (in kHz) | 1075 | 1875 | 2675 | 3475 | 4275 | 5075 | 5875 | 6675 | 7475 | 8075 | 9075 | 9875 | 10675 | 11475 | 12275 | 13075 | 13825 |

- The tests 10 (resp. 20) must coincide with the values obtained for the tests 11 (resp. 21), for the 20 or 30 dB steps as the case may be:

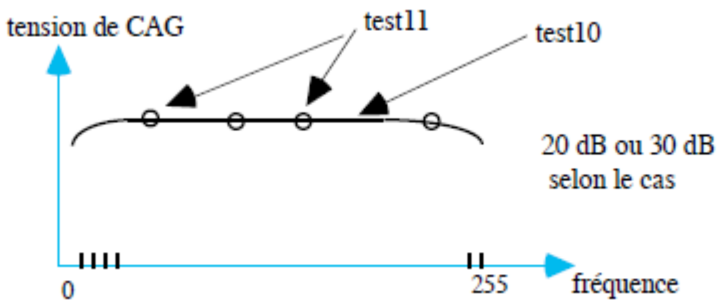


- We have 8 measurement points for each 2 dB step, that is to say 8 x s 0,358= 2,864 seconds per 2 dB step.

Note: the presence of a saturation zone, absent for the ULYSSES/URAP experiment, is a new fact of the WIND mission. However, for all the "log laws", the saturation zone has not been modeled. In the case of the Artemis project, for example, arctangent functions are used to do so.

Within the framework of the tests 11 and 21, other experiments are also implemented:

- Crosstalk: The receiver is necessarily in SEP mode with a single input signal.

- Z-hybrid: The receiver is necessarily in SUM mode.

- Sine: We use external generators G1 and G2 for a better accuracy in saturation. This test is performed for several frequencies.

## 5.5.3. Measuring the R-ratio: tests 12 and 22

The determination of the parameters characterizing a radio source (direction and polarization) requires the determination of the ratio $\tilde{R}$ (see [MAN80]), which appears in the equation giving the $P_S$ output power of the S track. We recall below how this ratio is introduced and how the parameters that constitute it are measured[7]:

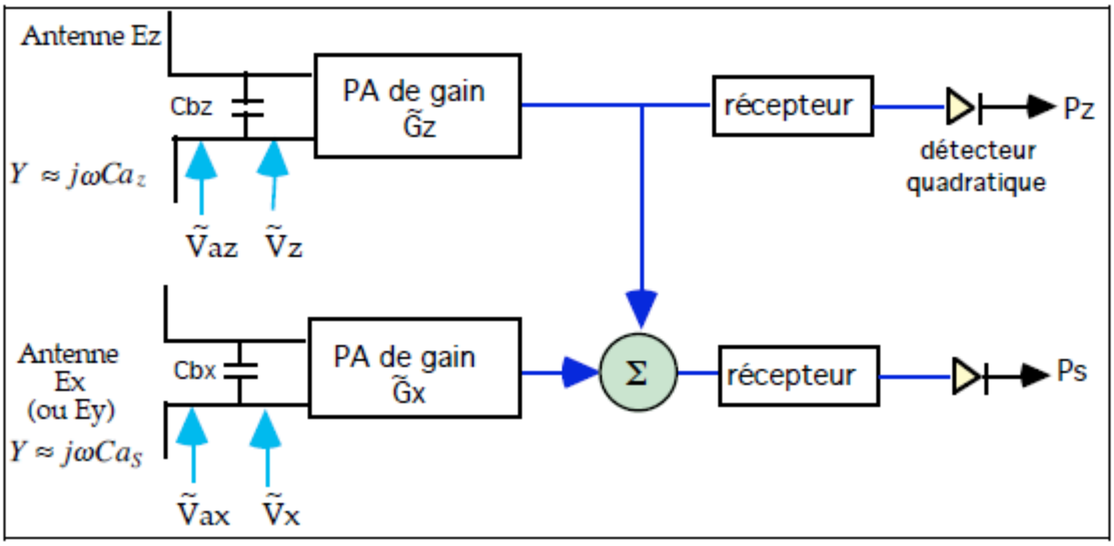


Fig. RAD1/2 receivers: input circuit

We consider below the case where we sum the inputs X + Z. The Y + Z is treated in the same way.

The gain of the system (PA + antenna) in channel S is written:

$$\tilde{g}_x = \tilde{G}_x \frac{Ca_x}{Ca_x + Cb_x} = \tilde{G}_x \cdot C_x'$$

Similarly, the system gain (PA + antenna) in channel Z is written:

$$\tilde{g}_Z = \tilde{G}_Z \frac{Ca_Z}{Ca_Z + Cb_Z} = \tilde{G}_Z \cdot C_Z'$$

The sign ~ indicates a complex quantity.

$C'_x$ (resp. $C'_z$ ) represents the "transfer function", between the terminals of the antenna $E_x$ (resp. of the antenna $E_z$), and the terminals of the PA. We have:

$$C_x' = \frac{Ca_x}{Ca_x + Cb_x} \qquad\qquad C_z' = \frac{Ca_z}{Ca_z + Cb_z}$$

[7] This chapter is extracted from an e-mail from R. Manning of 19/01/94.

$C_a$ and $C_b$ are the antenna and base (or parasitic) capacitances respectively. This ratio is only different from 1 due to the existence of the capacitance $C_b$ .

The output power of the channel S ( X + Z) is written:

$$P_S = < \left| \tilde{G}_z \tilde{V}_z + \tilde{G}_x \tilde{V}_x \right|^2 >$$

The symbol < > denotes a time average.

We still have :

$$P_S \propto \ < \left| \tilde{V}_z + \frac{\tilde{G}_x}{\tilde{G}_z} \cdot \tilde{V}_x \right|^2 > = < \left| V_z + \tilde{g}_x \cdot V_x \right|^2 >$$

We also have the following relations:

$$\tilde{V}_x = C_x' \cdot \tilde{V}a_x \quad \text{et} \qquad \tilde{V}_z = C_z' \cdot \tilde{V}a_z$$

From this it follows:

$$P_S \propto \ < \left| \tilde{V}a_z + \frac{C_x' \tilde{G}_x}{C_z' \tilde{G}_z} \tilde{V}a_x \right|^2 >$$

We also have the relationship between open circuit voltage and electric field, through the effective lengths:

$$\tilde{V}a_z = \tilde{E}_z \cdot L_z \quad \text{et} \qquad \tilde{V}a_x = \tilde{E}_x \cdot L_x$$

$\tilde{E}_x$ and $\tilde{E}_x$ are the projections of the electric fields incident on the $E_x$ and $E_z$ antennas respectively. $L_x$ and $L_z$ are the effective electrical lengths of the antennas $E_x$ and $E_z$, which are approximately half the corresponding physical lengths in the case of a dipole. So finally we have:

$$P_S \propto \ < \left| \tilde{E}_z + \frac{L_x C_x' \tilde{G}_x}{L_z C_z' \tilde{G}_z} \tilde{E}_x \right|^2 >$$

Thus, we see a ratio $\tilde{R}$ which is written:

$$\boxed{\tilde{R}_{xz} = \frac{L_x \cdot C'_x \cdot \tilde{G}_x}{L_z \cdot C'_z \cdot \tilde{G}_z}} \qquad \boxed{\tilde{R}_{yz} = \frac{L_y \cdot C'_y \cdot \tilde{G}_y}{L_z \cdot C'_z \cdot \tilde{G}_z}}$$

$\tilde{G}_x$, $\tilde{G}_y$ and $\tilde{G}_z$

are complex quantities that represent the voltage gain of the PA and the receivers to the summation point, for the X , Y and Z channels. Therefore, to estimate the ratio $\tilde{R}$ the antenna capacitances, their electrical length, and the receiver gain ratio must be known accurately.

The naming convention is as follows:

$$\tilde{G}_x = \left|\tilde{G}_x\right| \cdot e^{i \cdot \delta} \text{ et } \tilde{G}_z = \left|\tilde{G}_z\right|$$

So:

$$\frac{\tilde{G}_x}{\tilde{G}_z} = \left|\frac{\tilde{G}_x}{\tilde{G}_z}\right| \cdot e^{i \cdot \delta}$$

(same for y/z)

<u>Measurement of gain ratios</u>

The RAD1/2 receivers include a summation circuit (see diagram, chapter 3), which is an amplifier circuit with "inverting" input[8]. This circuit is such that if the same signal is applied to the inputs with the same sign, the output signal is zero. In practice we detect a minimum. Let us consider for example the channels X and Z and denote by $\tilde{x}$ the complex signal (amplitude, phase) sent to the X channel, and $\tilde{z}$ the complex signal sent to the Z channel. When the output of the summation circuit is zero, the following relationship is verified:

$$\tilde{x} \cdot \tilde{G}_x + \tilde{z} \cdot \tilde{G}_z = 0$$

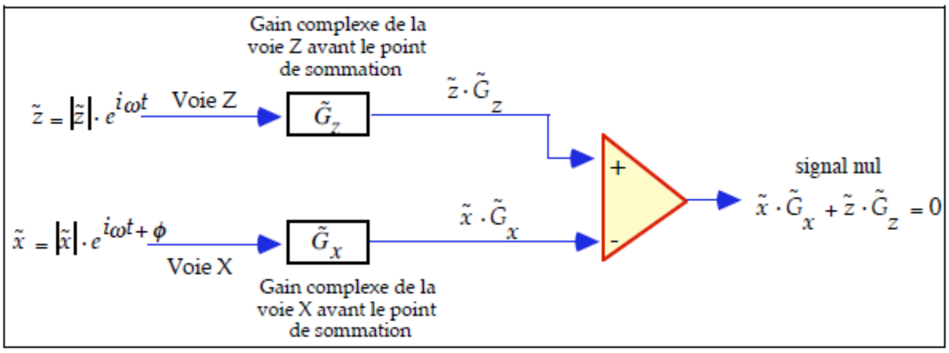


<u>Fig. Principle of the gain ratio measurement</u>

Let

$$\tilde{z} = |\tilde{z}| \cdot e^{i\omega t}$$

the input signal to channel Z, and

$$\tilde{x} = |\tilde{x}| \cdot e^{i\omega t + \phi}$$

[8] We remind that an ideal operational amplifier is characterized by an infinite voltage gain, an infinite input impedance, and an output impedance zero. The relationship between the inputs and the output of this circuit is written:
$\tilde{V}_0 = \tilde{A}_V(\tilde{V}_a - \tilde{V}_b)$ où $\tilde{A}_V$
is the voltage gain:

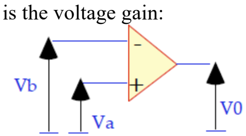


In the case of RAD1/2 receivers, the presence of an inverting input makes it possible to obtain a sum instead of a difference at the output of the amplifier.

the input signal to channel X, phase-shifted of $\Phi$ by the experimenter (see above) with respect to the signal $\tilde{z}$

Before summation, the input signal of channel X is

$$\tilde{G}_x \cdot |\tilde{x}| \cdot e^{i\omega t + \phi} = \left|\tilde{G}_x\right| \cdot |\tilde{x}| \cdot e^{i\delta} \cdot e^{i\omega t + \phi}$$

and the input signal to channel Z:

$$|\tilde{z}| \cdot \tilde{G}_z \cdot e^{i\omega t}$$

The condition of nullity after summation is written as follows:

$$\left|\tilde{G}_x\right| \cdot |\tilde{x}| \cdot e^{i\delta} \cdot e^{i\omega t + \phi} = -\left|\tilde{G}_z\right| \cdot |\tilde{z}| \cdot e^{i\omega t}$$

We have therefore by equalizing the modules:

$$\boxed{\left|\frac{\tilde{G}_x}{\tilde{G}_z}\right| = \left|\frac{\tilde{z}}{\tilde{x}}\right|}$$

The input amplitude ratio therefore provides the modulus of the gain ratio

$$\left|\tilde{G}_x / \tilde{G}_z\right| \text{ (ou } \left|\tilde{G}_y / \tilde{G}_z\right|)$$

at the frequency considered.

Similarly, by equalizing the phase terms, we obtain the phase shift between the X and Z channels:

$$e^{i\delta} \cdot e^{i\omega t + \phi} = -e^{i\omega t}$$

So:

$$\boxed{\delta = \pi - \phi}$$

The test 12 (respectively 22) consists in tracing the phase response of the RAD1 (respectively RAD2) receiver. To carry out this test, the RAD receivers are programmed in "freeze" mode (fixed frequency), and the responses S and S' of the receiver are observed as a function of the relative inputs X (or Y) and Z, for a given frequency at a time. The receivers are necessarily in SUM mode. We use a sinusoidal signal generator to generate the phase (which varies over a range of 360°)[9]. This is given with precision by the instrument. A priori, the most important variations observed are for the RAD2 instrument.

First, a signal is applied to the positive inputs: $+E_x$ (or $+E_y$) and $+E_z$, then to the negative inputs $-E_x$ (or $-E_y$) and $-E_z$. One of the two signals is kept constant while the other is varied in amplitude and phase, until a zero is obtained (this operation is rather delicate). The amplitude ratio and the phase difference between the two channels are noted and the results of the + and - inputs are averaged. The curves obtained have the following appearance:

[9] For this purpose, a generator is available which provides the amplitude, frequency and especially the phase of the generated signals with precision.

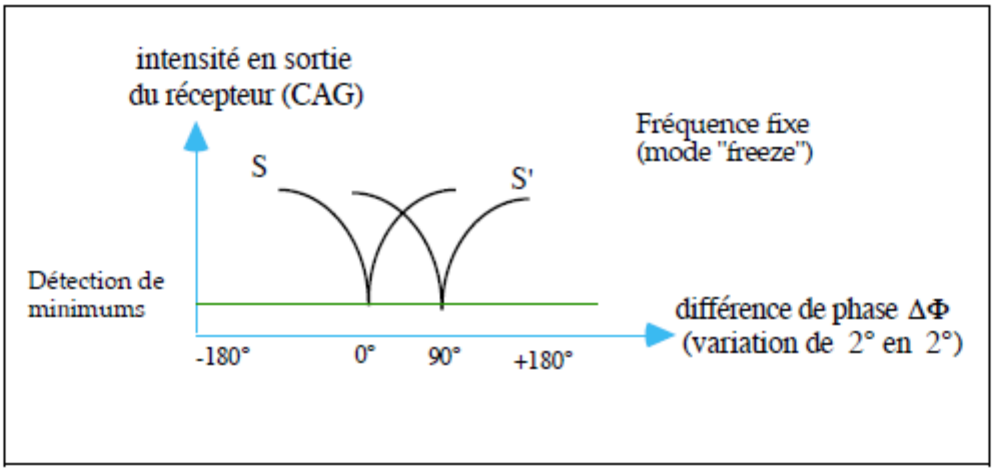


Fig. S and S' signals as a function of the phase difference between the X and Z channels

According to the measured curve and its complexity, the amplitude and phase of the gain ratio were measured for 16 to 28 different frequencies. A polynomial fit is performed using the MATLAB software. The best fits were obtained with polynomials of degree 4 or 5. We consider the following model:

$$\textit{Amplitude or phase} : c_0 + c_1 n + c_2 n^2 + c_3 n^3 + c_4 n^4 + c_5 n^5$$

where *n* represents one of the 256 possible frequencies. The polynomial coefficients obtained are the following:

Amplitude

| | RAD1 $E_x$-$E_z$ | RAD1 $E_y$-$E_z$ | RAD2 $E_y$-$E_z$ |
|---|---|---|---|
| $c_0$ | $2.7074453 \; 10^{-1}$ | $7.8678545 \; 10^{-1}$ | $8.7685044 \; 10^{-1}$ |
| $c_1$ | $6.7611007 \; 10^{-4}$ | $2.5636967 \; 10^{-4}$ | $-3.4445817 \; 10^{-4}$ |
| $c_2$ | $-3.5168039 \; 10^{-7}$ | $-8.7443445 \; 10^{-6}$ | $3.2029417 \; 10^{-5}$ |
| $c_3$ | $-1.2271751 \; 10^{-8}$ | $9.0838536 \; 10^{-8}$ | $-3.8278588 \; 10^{-7}$ |
| $c_4$ | $2.9771963 \; 10^{-11}$ | $-3.7589291 \; 10^{-10}$ | $1.6097720 \; 10^{-9}$ |
| $c_5$ | | $5.4737180 \; 10^{-13}$ | $-2.3195935 \; 10^{-12}$ |

<u>Phase</u>

| | RAD1 $E_x$-$E_z$ | RAD1 $E_y$-$E_z$ | RAD2 $E_y$-$E_z$ |
|---|---|---|---|
| $c_0$ | 1.6907392 $10^{+2}$ | 1.7022814 $10^{+2}$ | 1.8118782 $10^{+2}$ |
| $c_1$ | 2.8965931 $10^{-1}$ | -4.8895579 $10^{-3}$ | 9.8976373 $10^{-2}$ |
| $c_2$ | -3.1540504 $10^{-3}$ | 4.0415238 $10^{-4}$ | -1.9514405 $10^{-3}$ |
| $c_3$ | 1.3541357 $10^{-5}$ | -2.6738340 $10^{-6}$ | 1.1296770 $10^{-5}$ |
| $c_4$ | -2.0007034 $10^{-8}$ | 8.2812792 $10^{-9}$ | -1.9927228 $10^{-8}$ |
| $c_5$ | | -9.8347020 $10^{-12}$ | |

These coefficients allow us to build tables with 256 entries for the amplitude and phase of each gain ratio for each frequency channel. The values found for all 16 channels are given below:

<u>Adjusted values of the **amplitude** of the gain ratio by polynomial adjustment</u>

| canal fréquentiel | RAD1 $E_x$-$E_z$ | RAD1 $E_y$-$E_z$ | RAD2 $E_y$-$E_z$ |
|---|---|---|---|
| 0 | 2.7074453e-01 | 7.8703316e-01 | 8.7653763e-01 |
| 16 | 2.8142394e-01 | 7.8903229e-01 | 8.7850168e-01 |
| 32 | 2.9164902e-01 | 7.8856316e-01 | 8.8842546e-01 |
| 48 | 3.0118842e-01 | 7.8702712e-01 | 9.0046503e-01 |
| 64 | 3.0985761e-01 | 7.8537634e-01 | 9.1070641e-01 |
| 80 | 3.1751890e-01 | 7.8418268e-01 | 9.1687371e-01 |
| 96 | 3.2408142e-01 | 7.8370658e-01 | 9.1803727e-01 |
| 112 | 3.2950112e-01 | 7.8396596e-01 | 9.1432177e-01 |
| 128 | 3.3378081e-01 | 7.8480503e-01 | 9.0661437e-01 |
| 144 | 3.3697008e-01 | 7.8596322e-01 | 8.9627284e-00 |
| 160 | 3.3916538e-01 | 7.8714404e-01 | 8.8483367e-01 |
| 176 | 3.4050998e-01 | 7.8808396e-01 | 8.7372021e-01 |
| 192 | 3.4119397e-01 | 7.8862127e-01 | 8.6395081e-01 |
| 208 | 3.4145429e-01 | 7.8876496e-01 | 8.5584691e-01 |
| 224 | 3.4157467e-01 | 7.8876362e-01 | 8.4874121e-01 |
| 240 | 3.4188569e-01 | 7.8917427e-01 | 8.4068578e-01 |
| 255 | 3.4268539e-01 | 7.9075835e-01 | 8.2916564e-01 |

**Phase-adjusted** values of the gain ratio by polynomial fitting

| canal fréquentiel | RAD1 $E_x$-$E_z$ | RAD1 $E_y$-$E_z$ | RAD2 $E_y$-$E_z$ |
|---|---|---|---|
| 0 | 1.6907392e+02 | 1.7022365e+02 | 1.8128485e+02 |
| 16 | 1.7295519e+02 | 1.7024936e+02 | 1.8236029e+02 |
| 32 | 1.7553602e+02 | 1.7042025e+02 | 1.8271126e+02 |
| 48 | 1.7710200e+02 | 1.7068931e+02 | 1.8256643e+02 |
| 64 | 1.7790725e+02 | 1.7101998e+02 | 1.8212311e+02 |
| 80 | 1.7817443e+02 | 1.7138494e+02 | 1.8154727e+02 |
| 96 | 1.7809472e+02 | 1.7176487e+02 | 1.8097354e+02 |
| 112 | 1.7782784e+02 | 1.7214722e+02 | 1.8050520e+02 |
| 128 | 1.7750204e+02 | 1.7252495e+02 | 1.8021419e+02 |
| 144 | 1.7721409e+02 | 1.7289531e+02 | 1.8014113e+02 |
| 160 | 1.7702931e+02 | 1.7325860e+02 | 1.8029525e+02 |
| 176 | 1.7698154e+02 | 1.7361692e+02 | 1.8065448e+02 |
| 192 | 1.7707315e+02 | 1.7397297e+02 | 1.8116538e+00 |
| 208 | 1.7727506e+02 | 1.7432876e+02 | 1.8174319e+02 |
| 224 | 1.7752670e+02 | 1.7468439e+02 | 1.8227179e+02 |
| 240 | 1.7773603e+02 | 1.7503686e+02 | 1.8260372e+02 |
| 255 | 1.7778448e+02 | 1.7535791e+02 | 1.8257772e+02 |

The phase values are therefore within the following approximate ranges:

- RAD1 / $E_x$-$E_z$: 169° to 178° .
- RAD1 / $E_y$-$E_z$: 170° to 175°.
- RAD2 / $E_y$-$E_z$: 180° to 183°.

These values need to be confirmed by R. Manning.

The fitting curves are as follows: TBW.

It is also necessary to evaluate the ratio $C'_s/C'_z$ . This was measured as a function of frequency due to the stray inductance measured in the antenna mechanisms (refer to the general presentation). This shows that the amplitude of $C' = C'_x/C'_z$ or $C'_y/C'_z$ doesn't really depend on the frequency. In the worst case, the phase difference is -0.33 degrees for the highest RAD2 frequency. The values found are: $C'_x/C'_z = 2.133$ and $C'_y/C'_z = 1.328$.

When these values are calculated from the table in § 1-4/1-6, the values are close (TBD):

$$C'_x = \frac{Ca_x}{Ca_x + Cb_x} = 121{,}689/(121{,}689+20) = 0{,}8588 \qquad C'_y = \frac{Ca_y}{Ca_y + Cb_y} = 21{,}886/(21{,}886+20) = 0{,}522$$

$$C'_z = \frac{Ca_z}{Ca_z + Cb_z} = 25{,}30/(25{,}30+44) = 0{,}365$$

$$C'_x / C'_z = 0{,}8588/0{,}365 = 2{,}35 \qquad \text{et} \qquad C'_y / C'_z = 0{,}522/0{,}365 = 1{,}43$$

On the other hand, one must know the effective electrical lengths of the dipoles and the ratios $L_x/L_z$ and $L_y/L_z$. As the electrical lengths are not known, we can, as a first approach, use the physical lengths, that is

antenna $E_x$: 50 m, antenna $E_y$: 7.5 m, antenna $E_z$: 5.26 m.

Then we find: $L_x/L_z = 9.506$ and $L_y/L_z = 1.426$.

The ratios of the gains being given in the tables on the previous page, we have finally for RAD1:

$$\boxed{\left|R_{xz}\right| = \frac{L_x}{L_z} \cdot \frac{C'_x}{C'_z} \cdot \left|\frac{\tilde{G}_x}{\tilde{G}_z}\right| \approx 9{,}506 \cdot 2{,}133 \cdot (0{,}27 \text{ à } 0{,}35) \approx 5{,}5 \text{ à } 7{,}1}$$

$$\boxed{\left|R_{yz}\right| = \frac{L_y}{L_z} \cdot \frac{C'_y}{C'_z} \cdot \left|\frac{\tilde{G}_y}{\tilde{G}_z}\right| \approx 1{,}426 \cdot 1{,}328 \cdot (\approx 0{,}785) \approx 1{,}5}$$

<u>Important note</u>: The values of the electrical lengths and the R-ratio determined on the ground are only approximate. Indeed other factors influence (antenna in a plasma and not in vacuum, parasitic antenna capacities between the satellite body and the antenna, etc...). It is then necessary to estimate them more precisely in flight, by referring to known sources. An adjustment can be made from the observations to deduce R. By proceeding in this way, S. Hoang obtained the <u>value of 4.5 for the Ex antenna</u>.

In the phase-shifted case (output S'), it is sufficient to measure the amplitude and phase of this ratio at a single frequency because the summation is performed after the frequency change in the super-heterodyne receiver. Thus, the phase difference, *phase(S') – phase(S)*, for each input frequency must always be the same, from as well as the ratio of the amplitudes of the gain ratios between the out-of-phase and the in-phase cases, which was indeed verified.

Moreover, only two values are needed for RAD1, which can acquire the signal from $E_x$ or $E_y$, because in the summation circuit it is not known whether the receiver is connected to the $E_x$ or $E_y$ antenna. The values found for the amplitude correction term and the phase difference are:

| | $amplitude(S')/amplitude(S)$ | $phase(S') - phase(S)$ |
|---|---|---|
| RAD1 | 0.76° | -87.4° |
| RAD2 | 0.87° | 94.8° |

### 5.5.4. TNR receiver response to white noise: digital spectrum (test 30)

Test 30 consists of plotting the frequency response of the TNR receiver. It is thus to trace a spectrum, which has the following appearance:

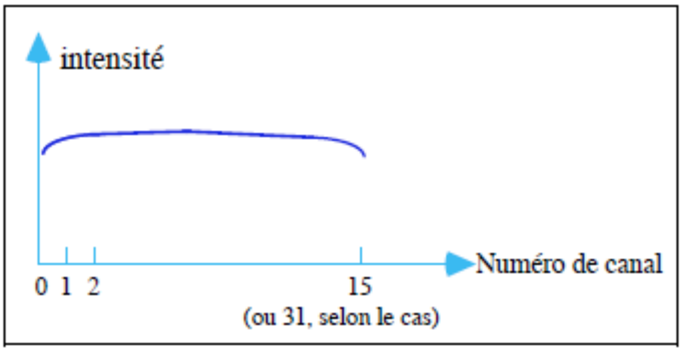


Fig. Test 30: calibration of TNR channels

- The GB is used, with a fixed attenuation level (40 dB for the $E_x$ antenna, 50 dB for the $E_y$ antenna, 50 dB for the $E_z$ antenna), in the GB band A, B, C, D, E, depending on the operating mode of the TNR receiver. No attenuation is applied to the R/B: the pass is direct.

- We consider the two receivers TNRA and TNRB.

- We consider 8 combinations of antennas (see table at the end of the §):

  $(+E_x,+E_y)$, $(+E_x,+E_z)$, $(+E_y,+E_x)$, $(+E_y,+E_z)$,

and the same with the - sign, that is: $(-E_x,-E_y)$ , $(-E_x,-E_z)$ , $(-E_y,-E_x)$ , $(-E_y,-E_z)$

- Mode: 2 (1 x 32 points), 3 (1 x 32 points), 4 (2 x 16 points).

We remind that these modes are the following:

| Mode | Receiver | Number of frequencies by spectrum |
|---|---|---|
| 2 | TNRA | 32 |
| 3 | TNRB | 32 |
| 4 | TNRA+TNR | 16 |

The number of curves obtained is:

Mode 2: (1receiver) x (8 antenna combinations) x (5 bands) = 40 curves.
Mode 3: (1receiver) x (8 antenna combinations) x (5 bands) = 40 curves.
Mode 4: (2receivers) x (8 antenna combinations) x (5 bands) = 80 curves.

Let: (40 + 40 +80) = 160 curves and (40 + 40 +40) = 120 steps.

The scheduling is as follows:

| Step | Mode | Antennas | Band |
|---|---|---|---|
| 0 | 2 | $+E_xE_y$ | A |
| 1 | 2 | $+E_xE_z$ | A |
| 2 | 2 | $+E_yE_x$ | A |
| 3 | 2 | $+E_yE_z$ | A |
| 4 | 3 | $+E_xE_y$ | A |
| 5 | 3 | $+E_xE_z$ | A |
| 6 | 3 | $+E_yE_x$ | A |
| 7 | 3 | $+E_yE_z$ | A |
| 8 | 4 | $+E_xE_y$ | A |
| 9 | 4 | $+E_xE_z$ | A |
| 10 | 4 | $+E_yE_x$ | A |
| 11 | 4 | $+E_yE_z$ | A |

Then the same sequence is executed for bands B (step 12 to 23), C (step 24 to 35), D (step 36 to 47), and E (step 48 to 59), making 5 x 12 = 60 steps. Then 60 other steps are executed with the same combinations of antennas, but with the sign -, which is the expected total of 120 steps.

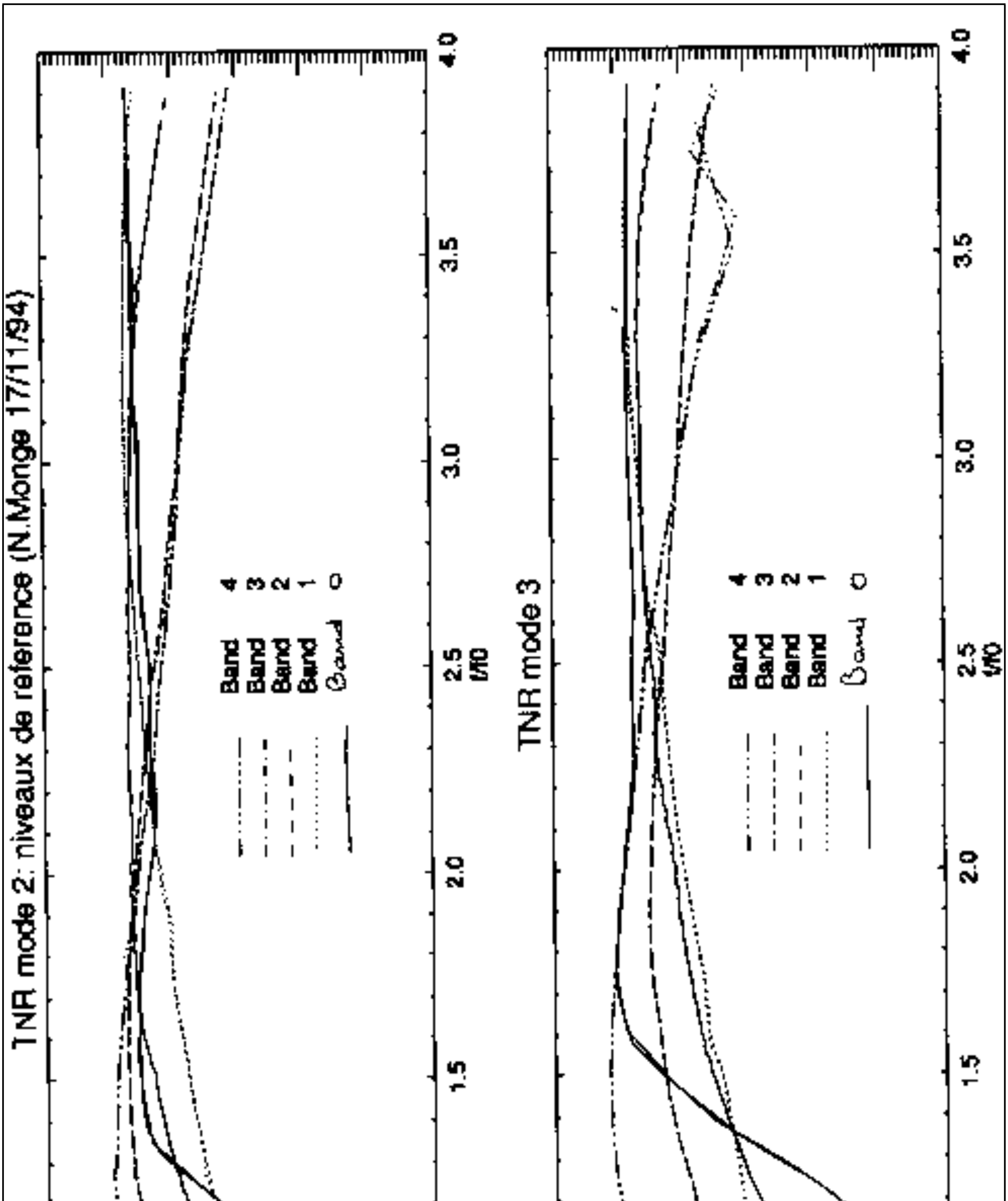


Test 30: Spectral Response

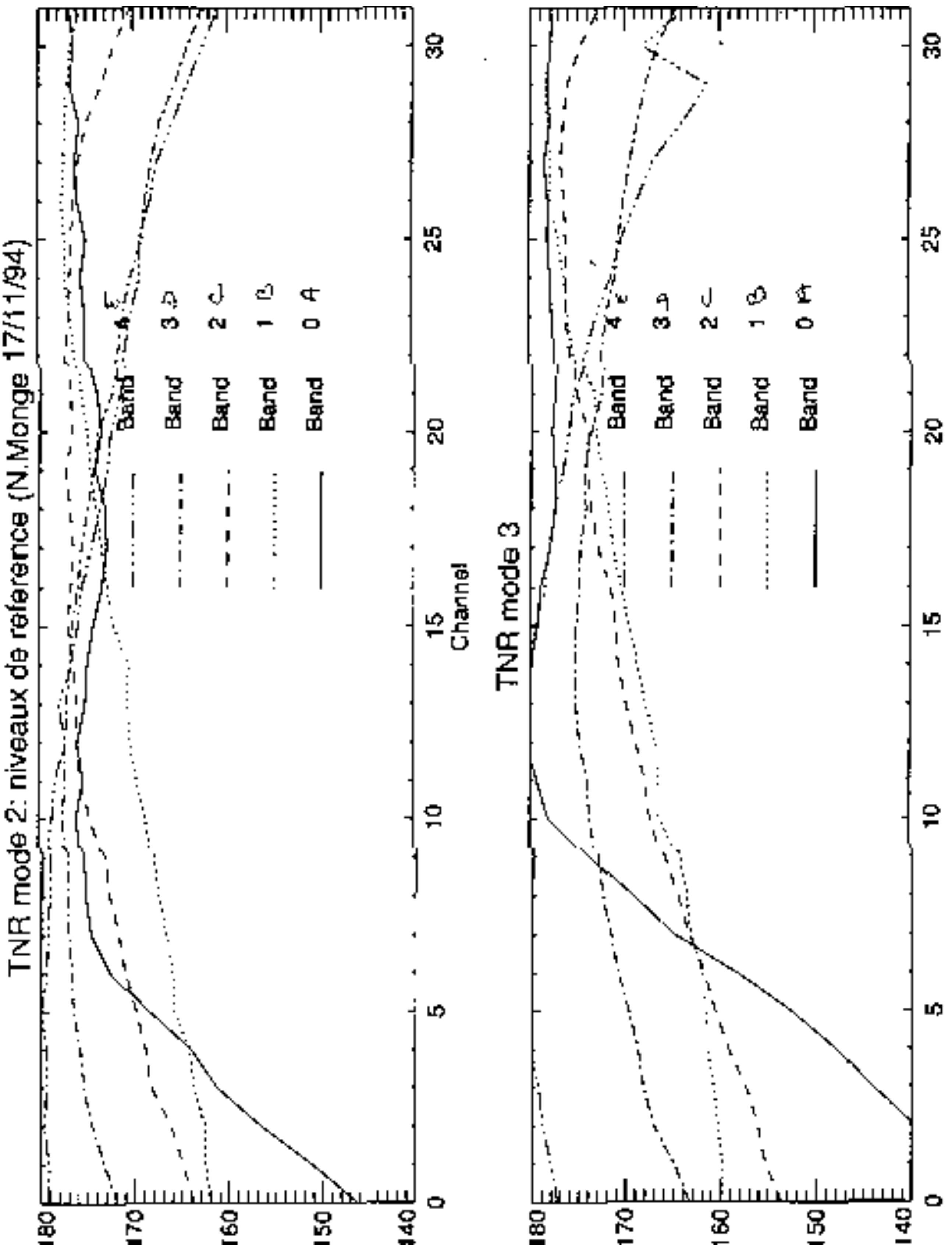

TNR mode 2: niveaux de reference (N.Monge 17/11/94)
Band 4 E
Band 3 D
Band 2 C
Band 1 B
Band 0 A
Channel
TNR mode 3
Band 4 E
Band 3 D
Band 2 C
Band 1 B
Band 0 A

### 5-5-5. TNR receiver amplitude response: test 31

Test 31 consists of plotting the amplitude response of the TNR receiver. In the terminology of the previous §, its purpose is to plot the curve giving $dB_{att}$ from a value of AGC at the output of the digital receiver. The calibration curve obtained has the following appearance:

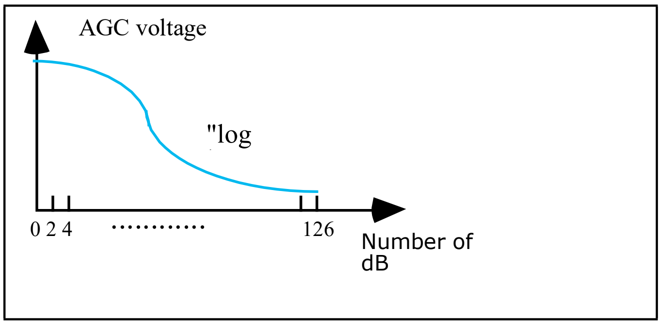


Fig. Test 31

- The GB is used with a variable level of 0 to 126 dB in steps of 2 dB.

- Such a curve is edited per antenna, per receiver and per band, and the parameters $A_1$, $A_2$, $A_3$, $A_4$ of the "log law" (see above) are determined by numerical adjustment, so in principle we have: 3 antennas x 2 receivers x 5 bands = 30 curves, but the TNRA is not connected to the $E_z$ antenna, so we only have 25 curves, so 25 quadruplets ($A_1$, $A_2$, $A_3$, $A_4$).

The measurements of these 25 quintuplets, used by the WIND/Waves software library, are as follows (except $A_4$):

| | | TNRA | | | TNRB | | |
|---|---|---|---|---|---|---|---|
| | | $A_1$ | $A_2$ | $A_3$ | $A_1$ | $A_2$ | $A_3$ |
| Antenna $E_x$ | Band A | 107,17 | 108,33 | 13,68 | 114,46 | 107,67 | 11,52 |
| | Band B | 112,44 | 106,64 | 14,29 | 106,06 | 105,05 | 32,54 |
| | Band C | 115,87 | 106,76 | 10,22 | 107,02 | 103,49 | 44,77 |
| | Band D | 117,05 | 106,58 | 10,24 | 103,88 | 100,91 | 63,12 |
| | Band E | 115,74 | 110,60 | 6,55 | 97,29 | 97,02 | 82,34 |
| Antenna Ey | Band A | 117,253 | Same values as for the antenna $E_x$ | Same values as for the antenna $E_x$ | 114,46 | Same values as for the antenna $E_x$ | Same values as for the antenna $E_x$ |
| | Band B | 122,656 | | | 106,06 | | |
| | Band C | 125,291 | | | 107,02 | | |
| | Band D | 126,026 | | | 103,88 | | |
| | Band E | 124,242 | | | 97,29 | | |
| Antenna $E_z$ | Band A | Not applicable | | | 115,777 | Same values as for the antenna $E_x$ | Same values as for the antenna $E_x$ |
| | Band B | | | | 107,008 | | |
| | Band C | | | | 108,054 | | |
| | Band D | | | | 104,713 | | |
| | Band E | | | | 98,103 | | |

Many values are identical: note that the coefficients $A_2$ and $A_3$ do not depend on the antenna $E_x$ or $E_y$ or $E_z$. Let us specify that these values are the result of a numerical adjustment which is delicate (see § 5-6). This determination is therefore highly susceptible to change.

## 5-5-6 Physical magnitude of a TNR digital spectrum

We present in this paragraph the method of deriving in physical quantities of the data collected in flight, at the output of the digital receiver. These developments have for support the electronic messages of 11/10/93 and 2/1/95 of R. Manning [MAN95]. The data measured in flight at the output of the TNR instrument include on the one hand a value of AGC (included between 0 and 255) as well as a numerical spectrum, noted $N_{mes}(i)$, where $i$ is the number of filter (0 to 15 or 0 to 31 according to the case).

- The parameters $A_1$, $A_2$ , $A_3$ , $A_4$ of the calibration curve $dB_{att} = f\,(GAC, A_1, A_2, A_3, A_4)$ , are determined on the ground before launch, by numerical adjustment, by means of a white noise generator (test 31 and §5-6).

From the telemetered AGC value on the one hand, and from the previous curve on the other hand, we determine the $dB_{att}$ value.

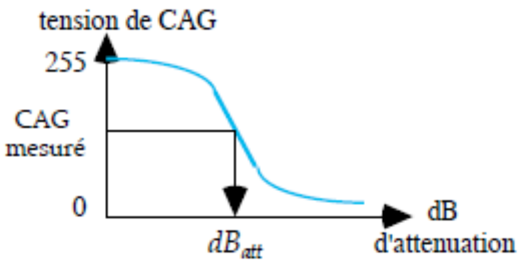


- The $dB_{entrée}$ value of the signal in the plasma at the input of the receiver, integrated over the entire current TNR band, is related to $dB_{att}$ by the equation

$$dB_{att} = dB_{V_0} - dB_{entrée} = 10\log_{10}\left(\frac{V_0}{V_{entrée}}\right)^2$$

Where $dB_{V0}$ is the value in dB of the reference voltage $V_0$, i.e. the unattenuated noise voltage, measured independently during the calibrations (see § 5-4). This $dB_{V0}$ depends only on the frequency band, and to a much lesser extent, the in-band filter (this is due to the cardinal sine shape of the frequency response of the noise generator).

- We acquire on the ground before launching, the digital values of telemetry between 0 and 255 noted, $N_{cal}(i)$, where $i$ is one of the 16 or 32 channels: it is the test 30. Indeed, it is necessary to take into account the way in which the power $V^2_{entrée}$ , in input of the receiver, is distributed in the various digital filters.

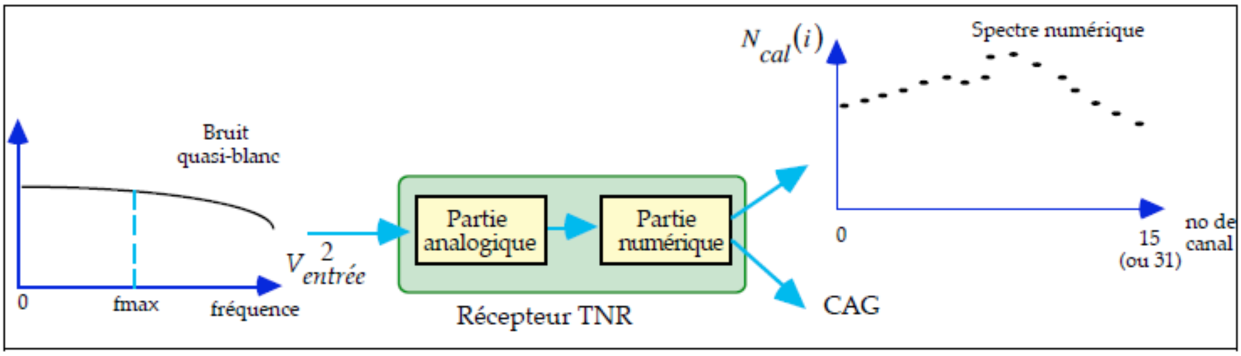


Fig. The digital spectrum from the receiver in response to white noise is not flat

In principle, since we are dealing with a white noise generator at the input of the receiver, the output power should be the same for all frequencies (flat spectrum), but this is not quite the case in practice. The values collected in flight in each channel will have to be weighted by these quantities $N_{cal}(i)$ which result from several effects:

- The width of the digital filters depends on the number of the filter in the band.

- The gains of the analog parts (remember that there is an analog circuit per frequency band) vary slightly with the frequency.

- The coefficients of the filters have been adjusted so that they can be contained as well as possible in the ROMs to 8 bits (TBV).

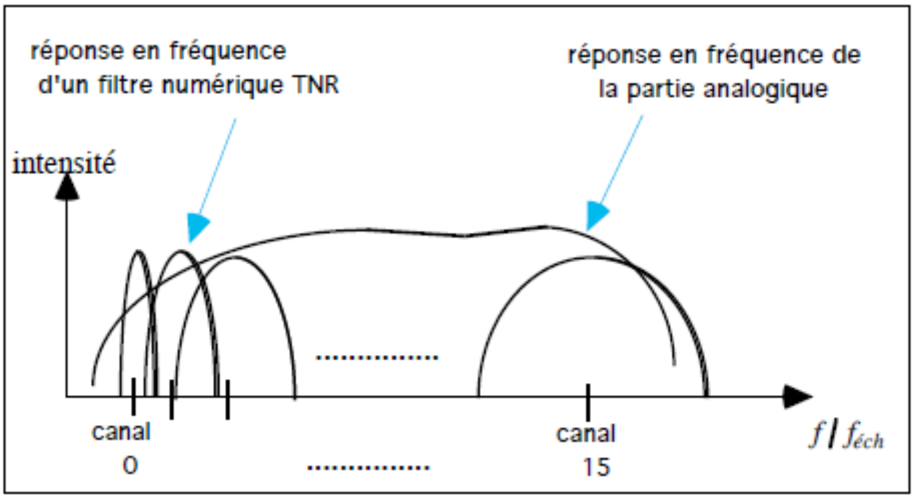


Fig. Frequency response of the analog part and the digital filters

From this point of view, in order to avoid the phenomena of saturation and background noise of the AGC amplifiers, we consider an average value of the attenuation of the GB and we place ourselves in the linear[10]

[10] The exact position in the linear region is not very important: in principle, the AGC circuit provides an output signal whose RMS value is constant whatever the level of the input signal, so the values in each channel will be the same whatever the attenuation. Here we have taken 40 dB.

region of the curve:

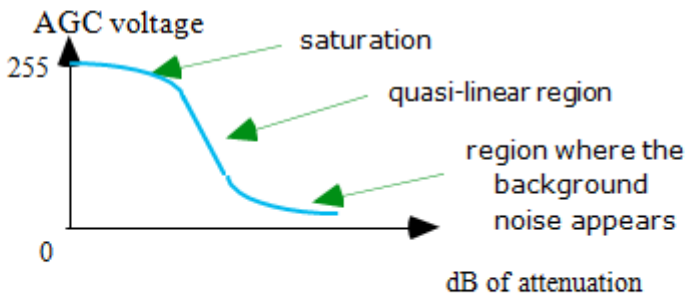


The plots below-TBW obtained at the output of the digital circuit for a value of AGC equal to TBC, show the effect of cut-off of the analog part for the extreme bands A and E and, in general, a growth of the values, due to the logarithmic evolution of the width of the channels

- Let the digital spectrum (telemetry values between 0 and 255) measured in flight noted $N_{mes}(i)$. These values must be weighted by the values $N_{cal}(i)$ , where $i$ is one of the 16 or 32 channels. Finally, we can reconstruct the spectrum in the plasma $V^2_{entrée}(i)$ using the following relation:

$$V^2_{entrée}(i) = \frac{V_0^2}{V_{att}^2} \cdot \frac{N_{mes}(i)}{N_{cal}(i)} = \frac{V_0^2}{V_{att}^2} \cdot T(i) \qquad 0 \le i \le 15 \;\; ou \;\; 0 \le i \le 31$$

or:

$$\boxed{dB_{entrée}(i) = dB_{V_0} - dB_{att} + dB_{mes}(i) - dB_{cal}(i)}$$

With, taking into account the digital compression of the telemetered values (see chapter on the TNR instrument):

$$\boxed{\begin{array}{l} N_{mes}(i) = 2^{\left(E_1(i)-3\right)}\left(8 + M_1(i)\right) \quad 0 \le i \le 15 \;\; ou \;\; 0 \le i \le 31 \\ N_{cal}(i) = 2^{\left(E_2(i)-3\right)}\left(8 + M_2(i)\right) \quad 0 \le i \le 15 \;\; ou \;\; 0 \le i \le 31 \end{array}}$$

$E_1(i)$ *and* $M_1(i)$ are the exponent and mantissa parts of the signal measured in flight $N_{mes}(i)$.

$E_2(i)$ *and* $M_2(i)$ are the exponent and mantissa parts of the reference signal $N_{cal}(i)$.

The two previous boxes gather the formulas used for the reconstruction of a TNR spectrum in physical quantities. In summary, we have:

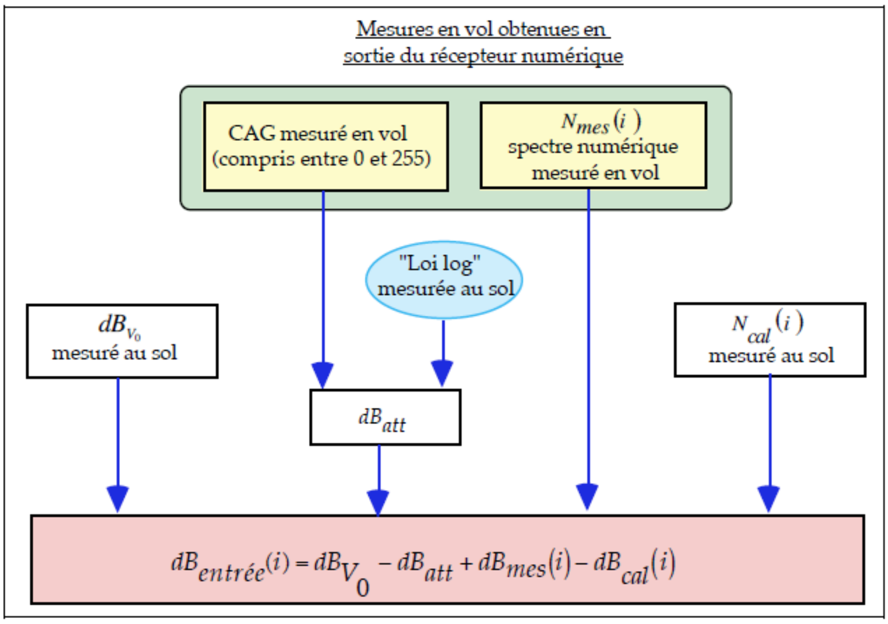


Fig. Physical unit derivation of TNR data

Form

| Symbol | Signification | Value in dB associated |
|---|---|---|
| $V_0$ | Noise voltage of the GB without attenuation. Value calculated theoretically or measured by summing the lines of the GB | $dB_{V_0} = 10\log_{10} V_0{}^2$ |
| $V_{entrée}$ | Input voltage of the receiver, integrated over the frequency range, measured on the ground. | $dB_{entrée} = 10\log_{10} V_{entrée}{}^2$ |
| $V_{att}$ | Attenuation voltage corresponding to the AGC value read in the telemetry. | $dB_{att} = dB_{V_0} - dB_{entrée} = 10\log_{10}\left(\frac{V_0}{V_{entrée}}\right)^2$ |
| $V_{entrée}(i)$ | Synthetic signal returned as a physical quantity at the input of the receiver, for the digital filter $i$ . | $dB_{entrée}(i) = dB_{V_0} - dB_{att} + dB_{mes}(i) - dB_{cal}(i)$ |
| $N_{cal}(i)$ | Value (between 0 and 255) measured on the ground, at the output of the receiver, for the filter $i$ : $N_{cal}(i) = 2^{(E_2(i)-3)}(8 + M_2(i))$ | By definition, we pose: $dB_{cal}(i) = 20\log_{10}(N_{cal}(i))$ |
| $N_{mes}(i)$ | Value (between 0 and 255) obtained in flight, at the output of the receiver, for the filter $i$ . | By definition, we pose: |
| $E_1(i)$ , $M_1(i)$ | Exponent and mantissa of the values of spectrum $N_{mes}(i)$ measured in flight. Values read in the telemetry. | Not applicable |
| $E_2(i)$ , $M_2(i)$ | Exponent and mantissa of the values of spectrum $N_{cal}(i)$ measured in flight. Values read in the telemetry. | Not applicable |

On R. Manning's URAP directory or, on the "megasr" machine, in the directory level: /wind1/waves_1/tnr, you can find the files giving $dB_{cal}(i)$, for each of the 5 frequency bands and the 16 or 32 filters, in the form:

A B C D E
Channel 0
Channel 1
.
.
.
Channel 30
Channel 31

The files have the following names:

| Mode | Antenna | Sub-receiver | file name |
|---|---|---|---|
| | Ex | TNRA | dbcal_2x.dat |
| 2 | Ey | TNRA | dbcal_2y.dat |
| 3 | Ex | TNRB | dbcal_3x.dat |
| 3 | Ey | TNRB | dbcal_3y.dat |
| 3 | Ez | TNRB | dbcal_3z.dat |
| 0 or 4 | Ex | TNRA | dbcal_4ax.dat |
| 0 or 4 | Ey | TNRA | dbcal_4ay.dat |
| 1 or 4 | Ex | TNRB | dbcal_4bx.dat |
| 1 or 4 | Ey | TNRB | dbcal_4by.dat |
| 1 or 4 | Ez | TNRB | dbcal_4bz.dat |

As an example, we present below the file dbcal_2x.dat:

| Channel | Band A | Band B | Band C | Band D | Band E |
|---|---|---|---|---|---|
| 0 | 6.4535123e+01 | 6.9950135e+01 | 7.0976828e+01 | 7.4038769e+01 | 7.6651949e+01 |
| 1 | 6.6199062e+01 | 7.0228718e+01 | 7.1466251e+01 | 7.4462603e+01 | 7.6795952e+01 |
| 2 | 6.8027176e+01 | 7.0531365e+01 | 7.1923082e+01 | 7.4758612e+01 | 7.6938513e+01 |
| 3 | 6.9771208e+01 | 7.0857601e+01 | 7.2409424e+01 | 7.5084707e+01 | 7.7041052e+01 |
| 4 | 7.1464288e+01 | 7.1060682e+01 | 7.2929378e+01 | 7.5254583e+01 | 7.7065178e+01 |
| 5 | 7.2970732e+01 | 7.1384712e+01 | 7.3334223e+01 | 7.5537311e+01 | 7.7125060e+01 |
| 6 | 7.4199669e+01 | 7.1791258e+01 | 7.3682811e+01 | 7.5750925e+01 | 7.7073320e+01 |
| 7 | 7.4862346e+01 | 7.2039073e+01 | 7.4093063e+01 | 7.5908710e+01 | 7.7010333e+01 |
| 8 | 7.5379209e+01 | 7.2207919e+01 | 7.4440404e+01 | 7.6042298e+01 | 7.6907195e+01 |
| 9 | 7.5545234e+01 | 7.2563873e+01 | 7.4766877e+01 | 7.6083809e+01 | 7.6772841e+01 |
| 10 | 7.5730476e+01 | 7.2833447e+01 | 7.5001683e+01 | 7.6176260e+01 | 7.6647087e+01 |
| 11 | 7.5492601e+01 | 7.3176729e+01 | 7.5150133e+01 | 7.6180761e+01 | 7.6493349e+01 |
| 12 | 7.5282820e+01 | 7.3431289e+01 | 7.5338362e+01 | 7.6091271e+01 | 7.6295639e+01 |
| 13 | 7.5175567e+01 | 7.3616488e+01 | 7.5561244e+01 | 7.6033567e+01 | 7.6127345e+01 |
| 14 | 7.5001130e+01 | 7.3881146e+01 | 7.5691112e+01 | 7.5863118e+01 | 7.5910597e+01 |
| 15 | 7.4842720e+01 | 7.4308861e+01 | 7.5818592e+01 | 7.5811770e+01 | 7.5710303e+01 |
| 16 | 7.4846576e+01 | 7.4397937e+01 | 7.5963727e+01 | 7.5670626e+01 | 7.5430311e+01 |
| 17 | 7.4753506e+01 | 7.4645482e+01 | 7.6092933e+01 | 7.5460397e+01 | 7.5178694e+01 |
| 18 | 7.4628310e+01 | 7.4829742e+01 | 7.6074734e+01 | 7.5245637e+01 | 7.4924485e+01 |
| 19 | 7.4698113e+01 | 7.5036346e+01 | 7.6141358e+01 | 7.5040423e+01 | 7.4646150e+01 |
| 20 | 7.4843478e+01 | 7.5234794e+01 | 7.6171403e+01 | 7.4847743e+01 | 7.4426764e+01 |
| 21 | 7.4905353e+01 | 7.5456587e+01 | 7.6197150e+01 | 7.4548353e+01 | 7.4111274e+01 |
| 22 | 7.5054098e+01 | 7.5739658e+01 | 7.6181415e+01 | 7.4354563e+01 | 7.3866147e+01 |
| 23 | 7.5059769e+01 | 7.5968763e+01 | 7.6104865e+01 | 7.4073032e+01 | 7.3639096e+01 |
| 24 | 7.5193029e+01 | 7.6119807e+01 | 7.6023362e+01 | 7.3741573e+01 | 7.3363608e+01 |
| 25 | 7.5429200e+01 | 7.6293300e+01 | 7.6074018e+01 | 7.3543832e+01 | 7.3168231e+01 |
| 26 | 7.5476454e+01 | 7.6374248e+01 | 7.5972421e+01 | 7.3192705e+01 | 7.2903024e+01 |
| 27 | 7.5823265e+01 | 7.6561802e+01 | 7.5790805e+01 | 7.3020669e+01 | 7.2617074e+01 |
| 28 | 7.5967901e+01 | 7.6519105e+01 | 7.5460304e+01 | 7.2545170e+01 | 7.2138473e+01 |

## 5.6. Digital adjustment of the amplitude response of the receivers

### 5.6.1. Modeling of the receivers response

The interest of modeling[11] the response curve of the receivers is the following:

- on the one hand in the reduction of the number of parameters characterizing this curve: in this case the 4 parameters $A_1$, $A_2$, $A_3$, $A_4$, rather than 64 calibration curve points.

- on the other hand, if we know the physical meaning of the parameters, in the possibility of interpreting the electronic origin of a possible evolution of the instrumental response, detected by the in-flight calibrations.

The numerical adjustment concerns the tests 11, 21 and 31. It is a question of reporting the response in gain

[11] This modeling is apparently not well understood in detail, which probably explains why it is not systematically implemented. The calibrations of the Cluster/STAFF experiment, for example, use instead a look-up table with 256 inputs.

(CAG) of the device with CAG of the receivers RAD1, RAD2 and TNR. The gain response curve of the receivers can be modeled mathematically as follows[12]:

$$\boxed{y = A_2 \log_{10}[(10^{(A_1-x)/10} + 10^{-A_4/10})^{1/4} - 1] + A_3} \quad (1)$$

$A_1$, $A_2$, $A_3$, $A_4$ are the calibration parameters. The AGC value is noted here as y. As a 8-bit telemetry is used, this value is between 0 and 255. The power 1/4 comes from the fact that we have two AGC circuits in cascade: with a single stage, we would have a power 1/2. The parameter $A_3$ has been introduced since the Ulysses/URAP experiment. The presence of this parameter is due to the fact that there is a small difference between the true *y* values and the values provided by the digitization chain. We also introduce the noise of the $A_4$ receiver.

| Symbol | Meaning | Dependency on f | Unit |
|---|---|---|---|
| x | Receiver input signal | - | dB of attenuation with respect to a $V_0$ reference voltage. |
| y | Output signal of the receiver (AGC voltage) | - | Telemetry unit (0 to 255) |
| $A_1$ | Total gain PA + receiver for a given AGC value (null) | Yes | dB |
| $A_2$ | Slope of the log law | No, depends on the receiver | Telemetry unit (0 to 255) |
| $A_3$ | DC offset voltage at IF stage | No | Telemetry unit (0 to 255) |
| $A_4$ | Receiver noise[13] + environmental noise | Yes | dB |

The ideal receiver without noise is represented by a law deduced from the previous one, by making $A_4$ tend to infinity, that is:

$$y = A_2 \log_{10}\left[10^{\left(A_1 - x\right)/40} - 1\right] + A_3 \quad (2)$$

[12] At DESPA, this function is often referred to as "log law" for short.

[13] This noise comes mainly from the PA. In the context of ground calibrations, the $A_4$ parameter depends, in addition to the receiver noise, on the experimental ambient conditions (mounting noise).

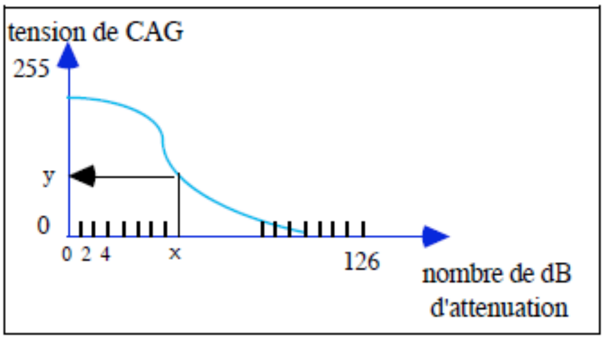


The telemetry values are related to the volts: the voltages from 0 to 5 Volts are coded from 0 to 255 on the ordinate, hence the 50 ratio between the Volts and the telemetry units.

### 5.6.2. Formulas of deriving physical quantities of the AGC

Inverting equation (2) from $y$ to $x$ , we obtain:

$$\boxed{x = A_1 - 40\left[\log_{10} 10^{(y-A_3)/A_2} + 1\right]} \qquad (3)$$

This is the equation used routinely for the physical value of the TNR receiver data, see test 30.

The quantity $x$ can then be converted into $V/\sqrt{Hz}$ using the equation

$$x_{dB} = 20\log_{10}\left(\frac{V_0}{V}\right)$$

where $V_0$ is the voltage corresponding to 0 dB of attenuation, which is also calibrated (see § 5-4 ).

Therefore, we have:

$$V = 10^{(-x/20)}\, V_0 \qquad (4)$$

Combining equations (3) and (4), we get:

$$\boxed{V(f) = 10^{\left[2\log_{10}\left(10^{(y-A_3)/A_2}+1\right)-\frac{A_1}{20}\right]} V_0(f)} \qquad (5)$$

This is the formula used for the derivation in physical quantities of the data of the RAD2 receiver. For this receiver, no 26 dB attenuation is applied (see § 5-2).

For the RAD1 receiver, on the other hand, the 26 dB of fixed attenuation must be taken into account:

$$26\ dB\ \log_{10}(att) \qquad \text{so:} \qquad att = 10^{26/20}$$

The final formula for the RAD1 receiver is therefore:

$$\boxed{V(f) = \frac{10^{\left[2\cdot\log_{10}\left(10^{(y-A_3)/A_2}+1\right)-\frac{A_1}{20}\right]}}{10^{26/10}} V_0(f)}$$

The output units of the data can be chosen differently: Volts, Volts$^2$, dB and $\mu V/\sqrt{Hz}$ (which induces positive or negative values), $nV/\sqrt{Hz}$ (which induces positive values), $V/\sqrt{Hz}$ (which induces negative values). For this experiment, the last option was chosen.

## 5.7. Internal calibration (test 4)

### 5.7.1. General

The purpose of the internal calibrations is to test a possible evolution of the response of the on-board receivers, in the various possible operating configurations of the instruments. These measurements are obviously less complete than the measurements of calibrations on the ground. The experiment has an internal noise generator for the needs of these calibrations. The pre-programmed sequence of "internal" or "in flight" calibration, also called "CAL sequence", occurs during the mission in a cyclic way at regular intervals, or can be triggered by remote command. The sequence of internal calibration orders is given below. By default, this sequence occurs every 24 hours, the first one occurring 4 hours after the reset[14]. The start of an internal calibration sequence is synchronized with an MF boundary (linked to the SCET), after the instrument cycles are completed. The calibrations of the Waves-1 and Waves-2 experiments occur in parallel, with the 32 first steps common to both. After the CAL sequence, the instruments begin new measurement cycles in the mode they were in before the sequence began. During the internal calibrations, the scientific data are not available[15].

Various programs for processing internal calibration data have been written (R. Manning and C. Perche).

These internal CAL sequences have also been implemented on the ground for testing purposes.

At the level of the WIND/Waves software library, the presence of internal calibration measurements can be tested by means of the item: CAL_FLAG (0: standard case, 1: internal calibration mode).

Table. Succession of the 60 internal calibration steps

[14] From now on, the time interval between two internal calibrations is 48 hours, the interval of 24 hours having been considered too restrictive.

[15] This is particularly visible on the dynamic spectra: a vertical white band is observed at this point.

| No calibration | Type | Selected entries | GB Clock | GB Att. Level | RAD1 antenna | SUM/SEP mode | TNR antennas | TNR mode |
|---|---|---|---|---|---|---|---|---|
| 0 | PA | +X+Y+Z | S | 7 | X | SUM | X-Y | 2 |
| 1 | PA | +X+Y+Z | S | 7 | X | SEP | X-Y | 2 |
| 2 | PA | +X+Y+Z | S | 7 | Y | SUM | X-Y | 3 |
| 3 | PA | +X+Y+Z | S | 7 | Y | SEP | X-Y | 3 |
| 4 | PA | -X-Y+Z | S | 7 | X | SUM | X-Y | 4 |
| 5 | PA | -X-Y+Z | S | 7 | X | SEP | X-Y | 4 |
| 6 | PA | -X-Y+Z | S | 7 | Y | SUM | Y-Z | 4 |
| 7 | PA | -X-Y+Z | S | 7 | Y | SEP | Y-Z | 4 |
| 8 | PA | +X+Y-Z | S | 7 | X | SUM | Y-Z | 4 |
| 9 | PA | +X+Y-Z | S | 7 | X | SEP | Y-Z | 4 |
| 10 | PA | +X+Y-Z | S | 7 | Y | SUM | X-Y | 4 |
| 11 | PA | +X+Y-Z | S | 7 | Y | SEP | X-Y | 4 |
| 12 | PA | -X-Y-Z | S | 7 | X | SUM | X-Y | 4 |
| 13 | PA | -X-Y-Z | S | 7 | X | SEP | X-Y | 4 |
| 14 | PA | -X-Y-Z | S | 7 | Y | SUM | Y-X | 4 |
| 15 | PA | -X-Y-Z | S | 7 | Y | SEP | Y-X | 4 |
| 16 | PA | +X+Y+Z | F | 7 | X | SUM | X-Y | 2 |
| 17 | PA | +X+Y+Z | F | 7 | X | SEP | X-Y | 2 |
| 18 | PA | +X+Y+Z | F | 7 | Y | SUM | X-Y | 3 |
| 19 | PA | +X+Y+Z | F | 7 | Y | SEP | X-Y | 3 |
| 20 | PA | -X-Y+Z | F | 7 | X | SUM | X-Y | 4 |
| 21 | PA | -X-Y+Z | F | 7 | X | SEP | X-Y | 4 |
| 22 | PA | -X-Y+Z | F | 7 | Y | SUM | Y-Z | 4 |
| 23 | PA | -X-Y+Z | F | 7 | Y | SEP | Y-Z | 4 |
| 24 | PA | +X+Y-Z | F | 7 | X | SUM | Y-Z | 4 |
| 25 | PA | +X+Y-Z | F | 7 | X | SEP | Y-Z | 4 |
| 26 | PA | +X+Y-Z | F | 7 | Y | SUM | X-Y | 4 |
| 27 | PA | +X+Y-Z | F | 7 | Y | SEP | X-Y | 4 |
| 28 | PA | -X-Y-Z | F | 7 | X | SUM | X-Y | 4 |
| 29 | PA | -X-Y-Z | F | 7 | X | SEP | X-Y | 4 |
| 30 | PA | -X-Y-Z | F | 7 | Y | SUM | Y-X | 4 |
| 31 | PA | -X-Y-Z | F | 7 | Y | SEP | Y-X | 4 |
| 32 | MF | (mf) | S | 5 | – | SUM | not applicable (cal MF) | 2 |
| 33 | MF | (mf) | S | 5 | – | SUM | | 2 |
| 34 | MF | (mf) | S | 5 | – | SUM | | 3 |
| 35 | MF | (mf) | S | 5 | – | SUM | | 3 |
| 36 | MF | (mf) | S | 7 | – | SEP | | 4 |
| 37 | MF | (mf) | S | 6 | – | SEP | | 4 |
| 38 | MF | (mf) | S | 5 | – | SEP | | 4 |
| 39 | MF | (mf) | S | 4 | – | SEP | | 4 |
| 40 | MF | (mf) | S | 3 | – | SEP | | 4 |
| 41 | MF | (mf) | S | 2 | – | SEP | | 4 |
| 42 | MF | (mf) | S | 1 | – | SEP | | 4 |
| 43 | MF | (mf) | S | 0 | – | SEP | | 4 |
| 44 | MF | (mf) | F | 5 | – | SUM | | 2 |
| 45 | MF | (mf) | F | 5 | – | SUM | | 2 |
| 46 | MF | (mf) | F | 5 | – | SUM | | 3 |
| 47 | MF | (mf) | F | 5 | – | SUM | | 3 |
| 48 | MF | (mf) | F | 7 | – | SEP | | 4 |
| 49 | MF | (mf) | F | 6 | – | SEP | | 4 |
| 50 | MF | (mf) | F | 5 | – | SEP | | 4 |
| 51 | MF | (mf) | F | 4 | – | SEP | | 4 |
| 52 | MF | (mf) | F | 3 | – | SEP | | 4 |
| 53 | MF | (mf) | F | 2 | – | SEP | | 4 |
| 54 | MF | (mf) | F | 1 | | SEP | | 4 |
| 55 | MF | (mf) | F | 0 | – | SEP | | 4 |
| 56 | BG | – | – | – | X | SUM | | 4 |
| 57 | BG | – | – | – | X | SEP | | 4 |
| 58 | BG | – | – | – | Y | SUM | | 4 |
| 59 | BG | – | – | – | Y | SEP | | 4 |

The experiment's internal noise generator provides 8 levels of attenuation relative to a reference voltage, spaced about[16] 8 dB apart. These levels are coded from 0 to 7. The noise spectrum is white in a certain frequency range:

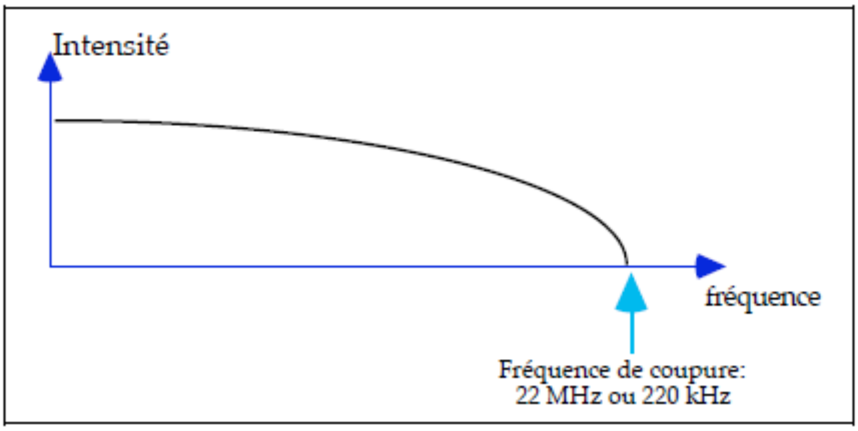


Fig. Noise spectrum of the internal generator

This spectrum extends from continuous to the following cut-off frequencies:

- for the fast clock frequency[17]: cut-off frequency F (Fast): 22 MHz.

- for the slow clock frequency: cut-off frequency S (Slow): 220 kHz.

For RAD and TNR receivers, the CAL sequence contains three main sections:

- CAL PA: calibration of the total response (PA + receiver). The purpose of this type of calibration is to anticipate the case where one of the PAs would see its operation deteriorate. The calibration takes place at the PA level, after the tracking stage. The X, Y and Z channels are isolated from the antennas by an R/B (electromechanical relay). The signal is fed to the PAs corresponding to the monopoles $+E_x$ or $-E_x$, or $+E_y$ or $-E_y$, etc..

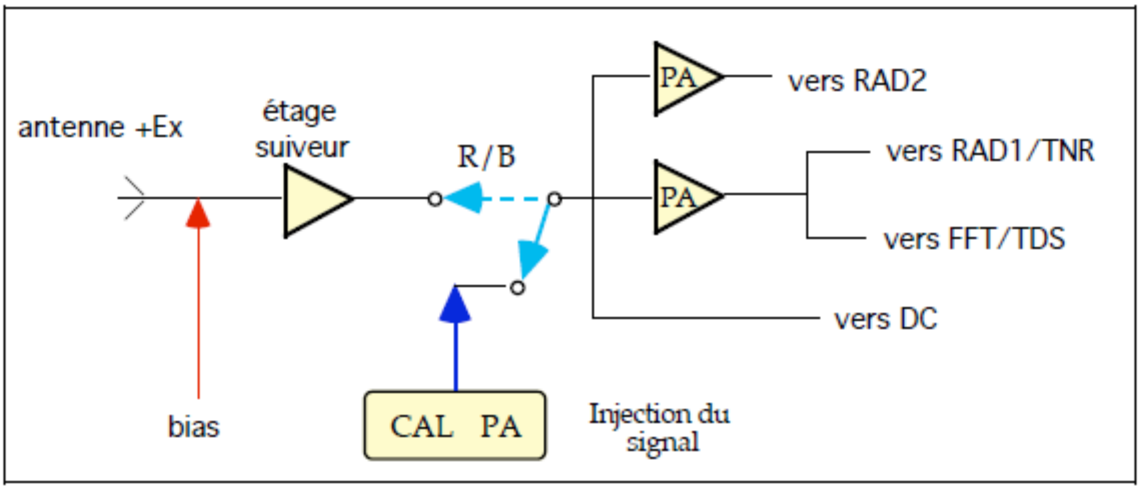


PA calibration in flight. Example of the +Ex antenna

[16] For RAD2, the difference is not always 8 dB, but the values are known.

[17] During the "fast" mode, it is rather the RAD1, RAD2 and TNR receivers in E band, that we study.

Calibration is done in gain, frequency and phase: only one fixed and high level of attenuation (of value 7, see table) is applied.

- CAL MF (medium frequency or intermediate frequency): calibration of the receivers alone. The calibration takes place directly at the input of the MF stages, at the output of the PAs, i.e. at the receivers. The PAs are isolated from the MF stages by an electronic switch located in the baluns/separator. The calibration is done in gain and phase: the 8 attenuation levels of the GB are successively applied to the input of the MF stages.

- "Background": at the end of the CAL sequence, a "background" (BG) measurement is carried out: this involves measuring the background noise in the absence of a signal. To do this, the internal noise generator is switched off.

Duration

The duration of an internal calibration step is 20 mf in LBR or 40 mf in HBR, that is:

(20 mf) x (0.368 seconds per mf) = **7.36 seconds**

During this time, we have: 7.36/1.472 = 5 TNR spectra (ABCDE).
7.36/0.358 ≈ 20 measurements RAD1: only 16 are used.
7,36/0.063 ≈ 116 measurements RAD2: only 6 x 16 are used.

We note a synchronism with the measurements of the TNR instrument. We recall that the integration time of a TNR spectrum is a multiple or sub-multiple of the duration of an mf. This is not the case for the RAD1/2 instruments.

The total duration of a calibration cycle is (LBR or HBR):

(60 internal calibration steps) x (20 mf) x (0.368 s per mf) = 60 x 7,36s = **7 mn 22 s.**

## 5.7.2. Configurations considered

The table in § 5-7-1 shows the sequence of 60 internal calibration steps (orders). The configurations considered are the following:

- SUM/SEP for RAD1/2 receivers.

- Antenna combinations: (+Ez,+Ex),(+Ez,-Ex),(+Ez,+Ey),(+Ez,-Ey),(-Ez,-Ex),(-Ez,+Ex)

Measurements in SUM mode with different antenna combinations allow phase control of the PAs as well as the receivers.

- TNR modes (see § 4-4) considered:

| | | |
|---|---|---|
| Mode 2 | TNRA | 32 frequencies per spectrum |
| Mode 3 | TNRB | 32 frequencies per spectrum |
| Mode 4 | TNRA + TNRB | 16 frequencies per spectrum<br>(16 frequencies of the TNRA, 16 frequencies of the TNRB) |

The implementation of the different configurations can be checked from the table in § 5-7-1. The composition of the columns in this table is as follows:

| | |
|---|---|
| 1st column | Calibration on PA or MF |
| 2nd column | 3 stimulated PAs among the 6 possible ones |
| 3rd column | Noise generator, Fast or Slow. |
| 4th column | Noise attenuation level (from 7 to 0) |
| 5th column | Antenna seen by RAD1 |
| 6th column | Summed mode (SUM) or not (SEP) (RAD1 and RAD2) |
| 7th column | Antennas seen by TNRA and TNRB respectively |
| 8th column | How the TNR works |

For example, at step nº 0:

- We use the three PAs: +Ex, +Ey, +Ez. Remember that there are six PAs for the +Ex monopoles respectively,
- -Ex, +Ey, -Ey, +Ez, -Ez.
- The GB operates at a slow rate (S) and its attenuation level is maximum (7).
- For the RAD1 receiver, the $E_x$ antenna is selected. Remember that the RAD1 receiver can be connected to the $E_x$ antenna or to the $E_y$ antenna.
- RAD1/2 receivers are in SUM mode.
- The TNRA receiver (resp. TNRB) acquires the signal from the $E_x$ input (resp. $E_y$).
- The TNR is in 2.
- N.B. The RAD2 receiver is always connected to the $E_y$ antenna. This explains why there is no column for this receiver in the table.

Frequencies used for RAD1/2 receivers

The frequencies used for the internal calibrations are equally distributed, with 8 frequencies for RAD1 and 16 frequencies for RAD2:

RAD1

| Frequency number | Frequency value (kHz) |
|---|---|
| 0 | 20 |
| 32 | 148 |
| 64 | 276 |
| 96 | 404 |
| 128 | 532 |
| 160 | 660 |
| 192 | 788 |
| 224 | 916 |

RAD2

| Number of frequency | Value of the frequency (MHz) |
|---|---|
| 0 | 1,075 |
| 16 | 1,875 |
| 32 | 2,675 |
| 48 | 3,475 |
| 64 | 4,275 |
| 80 | 5,075 |
| 96 | 5,875 |
| 112 | 6,675 |
| 128 | 7,475 |
| 144 | 8,275 |
| 160 | 9,075 |
| 176 | 9,875 |
| 192 | 10,675 |
| 208 | 11,475 |
| 224 | 12,275 |
| 240 | 13,075 |

Note: On ULYSSES/URAP, for example, there are 8 frequencies in CAL PA for in-flight calibration, 4 frequencies in CAL MF.

Synchronization curve

Example of experimental curves of internal calibration of the TBC instrument

## 5.8. Evaluation of the calibration tests

Several problems were encountered during the analysis of the WIND/Waves data, in particular concerning the TNR instrument. The TNR instrument is of new design. This has led to various problems, which were discussed in the course of the calibrations. The WIND/Waves software library which provides the data of the experiment in physical quantities, takes into account the evolutions in this field. We list below the problems identified and the attempts made to circumscribe and solve them.

### 5.8.1. TNR calibrations

#### 5.8.1.1. The observation of the problems

- **ADSP Programming**

A software error in the programming of the ADSP microprocessor distorted the results of the instrument calibration tests during the refurbishment phase at the University of Minnesota. The power spectra were accumulated in floating point registers using mantissa 16 bits: for a very high[18] number of accumulations, the last spectra were not counted ("underflow"). It is generally desirable to choose a long integration time to minimize the random fluctuations of the signals (cf. § 4-7) and this is the approach that was adopted. However, the error is all the more pronounced as the integration time is long, in particular for the E band, for which the number of averages is the highest. For the embedded software, this problem has been corrected in the form of a "patch" with an accumulation of spectra on 32 bits.

Two measurements were made in extremis, but one concerning the TNRA receiver was noisy (R. Manning says that the TNRB receiver is therefore better calibrated than the TNRA receiver). Therefore, the number of "log laws" collected for the TNR instrument is insufficient. An attempt is made to overcome this problem by using in particular the results of internal calibrations.

NB. For reasons related to the instrumental design, the A-band of the TNRB receiver does not work very well.

- **Limitation of the dynamics**

The A/D C digitizes the analog values into 8 bits[19], resulting in a digital dynamic range of 45 dB. A signal that does not fit within this dynamic range is lost:

[18] That is, in the worst case in E-band, mode 0 or 1, integration time 1,472 less, number of integrations = 1994.

[19] It would be desirable to have A/D C 16 or 32 bits, but for the high scanning speed required, such circuits are not yet available.

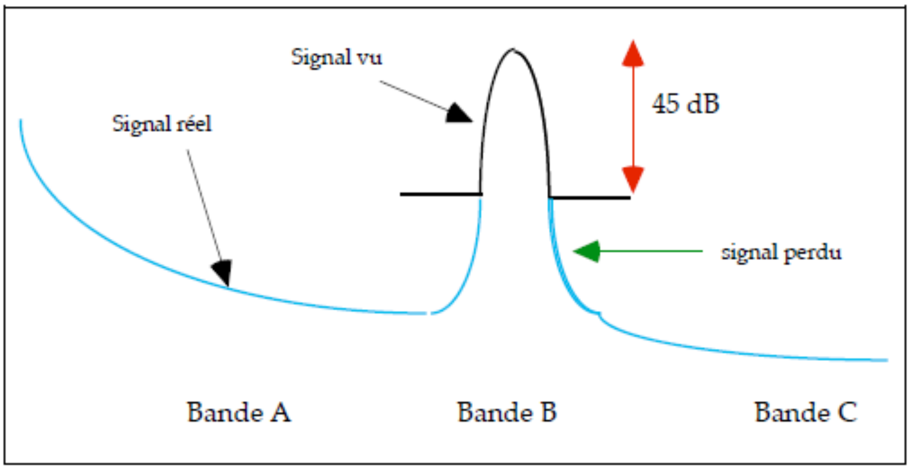


Fig. Signal loss due to dynamic range limitation of the receiver

Note however that, except for instabilities, a TNR spectrum does not exceed 45 dB of dynamic range. When the signal is such that the dynamic range is higher, there is clipping which generates spurious signals, spreading the spectra and raising the edges. This can lead to a problem with the connection between frequency bands. M.Maksimovic noted that a 1/2 dB error in the height spectrum can lead to a 40% error in the estimate of the electron temperature of the plasma.

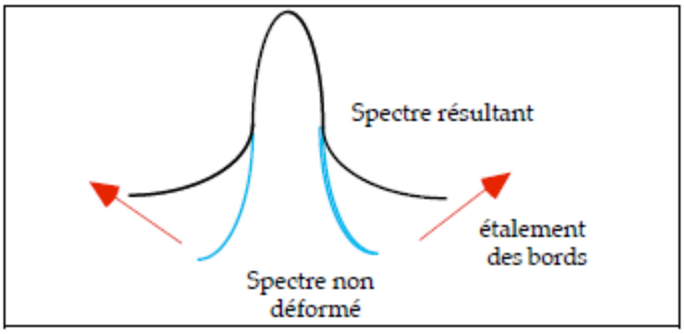


Fig. Spreading of the spectrum by generation of spurious signals

- **Fast signal detection**

Spectral analysis is power averaging: the successive AGC values are averaged. When the signal fluctuates rapidly, for example in the case of transient phenomena, the AGC circuit is not able to normalize the signal quickly enough: the loop does not have time to respond, especially for any event lasting less than about 25 ms.

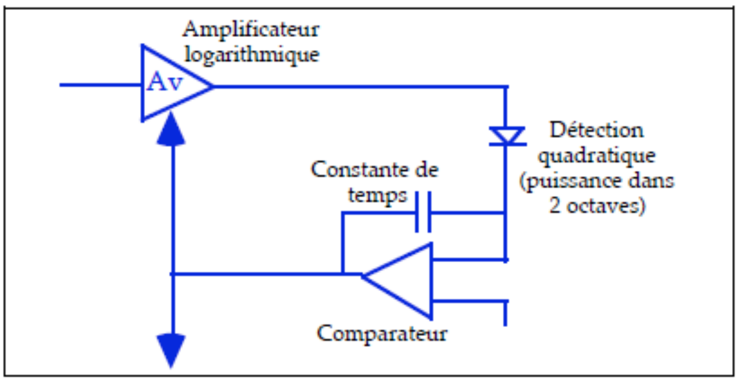


Fig. AGC loop and response time

The lowest frequency bands, especially the A-band which only samples the signal at 64 kHz, are the most sensitive to this phenomenon.

- **<u>Measurement uncertainties (dB0, dBcal, "log law" adjustment)</u>**

In addition to the $dB_{cal}(i)$ values, the sources of error in the TNR instrument calibrations can come from the uncertainty on the $dB_{V0}$ value (reference voltage without attenuation) and the difficult adjustment of the "log law" when the noise level is too high:

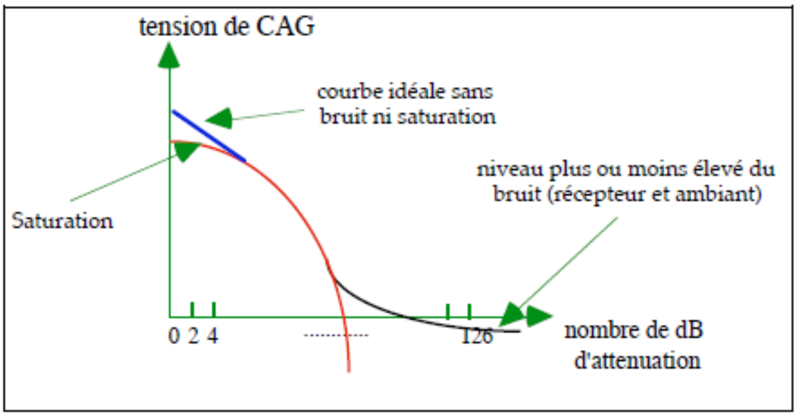


Fig. Noise level and saturation at the "log law" level

Noisy test equipment was used so that only curves that do not go low enough are available.

- **<u>Saturation of the GAC at 245</u>**

#### 5.2.1.2. Actions in progress

- **<u>TNR telemetry mode</u>**

For the time being, the instrument has been switched to ABCDE mode, TNRA receiver. R. Manning thinks that the dynamic spectra are better in TNRB (better behavior towards AKR). We can therefore try to switch to TNRB receiver. Obviously, the A-band of TNRB does not work well: this receiver was designed to be more sensitive, but it is not the case in practice. It would therefore be better to design the following combination:

| | |
|---|---|
| Band A | of the TNRA receiver |
| Bands B,C,D,E | of the TNRB receiver. |

For this, a new telemetry mode ("patch" of the DPU) must be considered: K. Goetz must write an assembler code for this, which must be tested beforehand on the Identification Model.

- **<u>First calibration test</u>**

The calibration coefficients obtained do not allow the bands to be connected (especially for the November28 curve). By using the curves where no saturation is observed, we try to find a common zero. The superposition obtained from the different curves is of good quality, with the same slope.

- **<u>Second calibration test (12 dB)</u>**

The calculations below are TBC.

We remind the expression of the "log law":

$$y = A_2 \log_{10}\left[\left(10^{(A_1-x)/10}+10^{-A_4/10}\right)^{1/4}-1\right]+A_3$$

If we carry the noise, represented by the parameter $A_4$ , into the input signal:

$$y = A_2 \log_{10}[10^{(A_1-x)/40}-1]+A_3$$

When $x \to -\infty$ ,

$$y \to A_2 \log_{10}[(10^{(A_1-x)/10})^{1/4}]+A_3$$

When $x \to -\infty$ , the "log law" is thus equivalent to a linear equation:

$$y = A_2 \cdot \frac{(A_1-x)}{40}+A_3$$

In particular, in $x = A_1$, $y = A_3$. Let $(x_0, y_0)$, be the point where the log law intercepts the dB axis of attenuation.

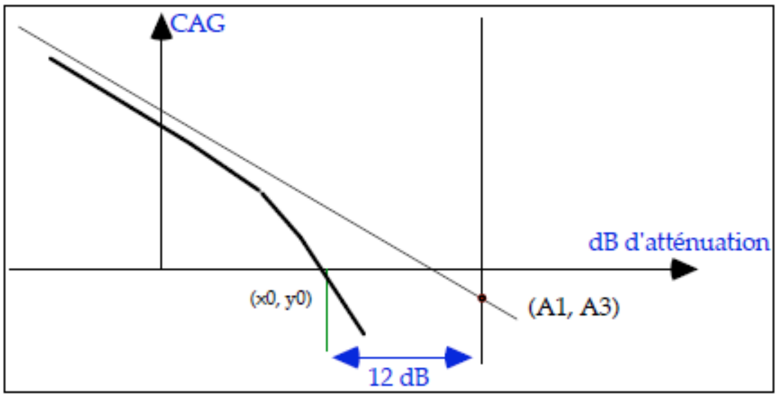


Fig.

Assuming: $\underline{A_1 - x_0 = 12\ dB}$, which is electronically justified, we have:

$$0 = A_2 \log_{10}[10^{12/40}-1]+A_3\text{, soit: } A_3 \approx 2 10^{-3} A_2 .$$

For a typical value of $A_2$ of 100, we find $A_3$ = 0,02 which is small: $A_3$ would have no role compared to the other sources of error.

This attempt to force $A_1 - x_0$ to 12 dB was not successful.

- **<u>Third calibration test: Modeling of test equipment imperfections</u>**

The test equipment introduces an additional phase:

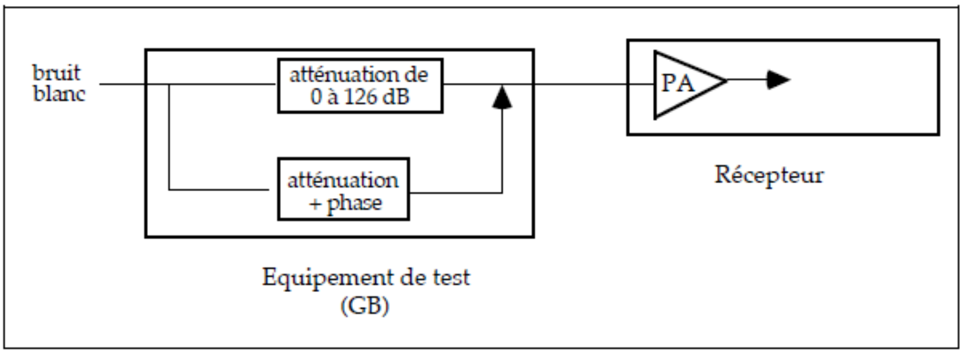


Fig. Leakage current

To take into account this leakage circuit, a new modeling is proposed:

If we pose: $u = (S + B)^{1/4} - 1$

with $S$ for Signal and $B$ for Noise,

The "log law" is rewritten as follows: $y = A_2 \log_{10(u)} + A_3$

In the new model, $S + B$ becomes:

$$S + B\left(1 + \sin^2 \theta\right) + 2\cos \theta \sqrt{SB}$$

So we have one more parameter in the numerical fit, i.e. 5 parameters. The fit works well in this case. The oscillations are attenuated by a factor of about 5 (the standard deviations are clearly reduced). When we use the coefficients obtained in this way, we see a fairly good agreement between bands A, B, C, D but not with the E band.

- **Fourth test: AGC level**

By definition of an AGC circuit, the average power at the AC/N input must always be the same, regardless of the input signal level. C. Perche found that sometimes the AGC circuit does not reach its equilibrium point. This is not the case in E-band. He therefore suggests compensating for this effect.

$$dB_{entrée}(i) = dB_{V_0} - dB_{att} + dB_{mes}(i) - dB_{cal}(i)$$

## 5-8-2 RAD1/2 Calibrations

The RAD1 receiver is calibrated correctly. The RAD2 receiver is more problematic[20].

The background noise of the receivers has been measured and we give below the corresponding curves. We observe in particular:

- For RAD1

[20] The higher the frequencies, the more delicate the design of the electronic circuits becomes (e.g. generation of parasitic capacities).

* At low frequencies, the effect is due to photoelectron noise and to an internal problem due to the instrumental design.

* The influence of high frequency galactic noise and the beginning of antenna resonance.

- <u>For RAD2:</u>

* A depression that can easily be interpreted as a resonance of the boom supporting the magnetometer. It is indeed precisely the resonance frequency of the magnetometer. The boom, placed at 45° to the Waves antenna, creates a symmetry defect, and it is reasonable to think that this has the effect of increasing the base capacity. There is little effect on the $E_z$ antenna.

* A first antenna resonance when it resonates with the base capacitance slightly after the 1/2 wave resonance frequency (we have already gone from capacitive to inductive). The high frequency signal level, especially the broadband noise centered at 12 MHz, is higher than expected. The background noise plot shows a "hump" at this frequency. The expression for the antenna resonance frequency is written: $f_{\lambda} = c/l$. That of the half-resonance is written: $f_{\lambda/2} = 2c/l$, where $l$ is the antenna length. In general, we work in a region close to the resonance. The resonance frequency for the RAD2 receiver, connected to the $E_y$ antenna (l = 2 x 7.5m), is therefore theoretically: $f_{\text{rés}} = 20MHz$.

In practice, we note that this resonance appears at 12 MHz, which poses a problem because the RAD2 receiver has an operating range from 1,075 MHz to 13,825 MHz. This phenomenon was noted after launching. Note that it would not be observed without the existence of basic capacity.

The basic capacitances (= parasitics) of the antennas have been measured on the ground. The following values were obtained: $E_x$, $E_y$ antenna: 20pF +/- 0.5 pF and $E_z$ antenna: 44 pF (with a slightly higher error bar).

It is possible that, due to the presence of the magnetometer boom, these values are higher. Desch (cf. internal report) made an adjustment at the location of this resonance by varying $C_b$: he finds the value 33 pF instead. M. Reiner and P. Kellog question the 33pF value, however, in view of the low frequency results. R. Manning thinks that we should have the same effect on RAD1 and RAD2.

In the ULYSSES/URAP experiment, the background subtraction provided a decent fit to the plasma line, which is not the case before subtraction. For the determination of the electron temperature and solar wind speed from the QTN analysis, subtraction of the best estimate of the background is an important operation.

The background noise can be determined using the results of internal calibrations done on the ground. It can also be determined by results obtained in flight with the antennas not deployed.

The shape of the noise changes with the amplitude of the signal (the noise passes through the receiver and is therefore influenced by its transfer function). With a good calibration, we could subtract this noise.

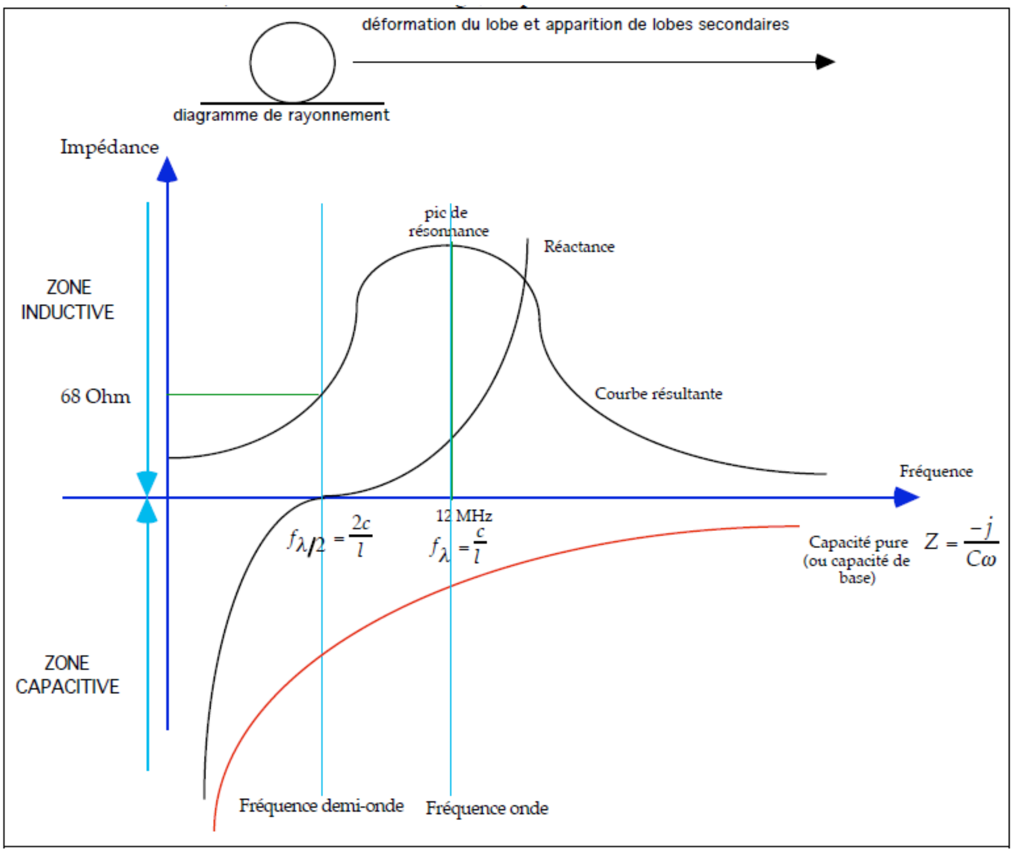

Fig. Antenna resonance peak for the RAD2 receiver.

The antenna impedance is the resultant of the reactance and the base and antenna capacities. The resultant curve is shown in this figure.

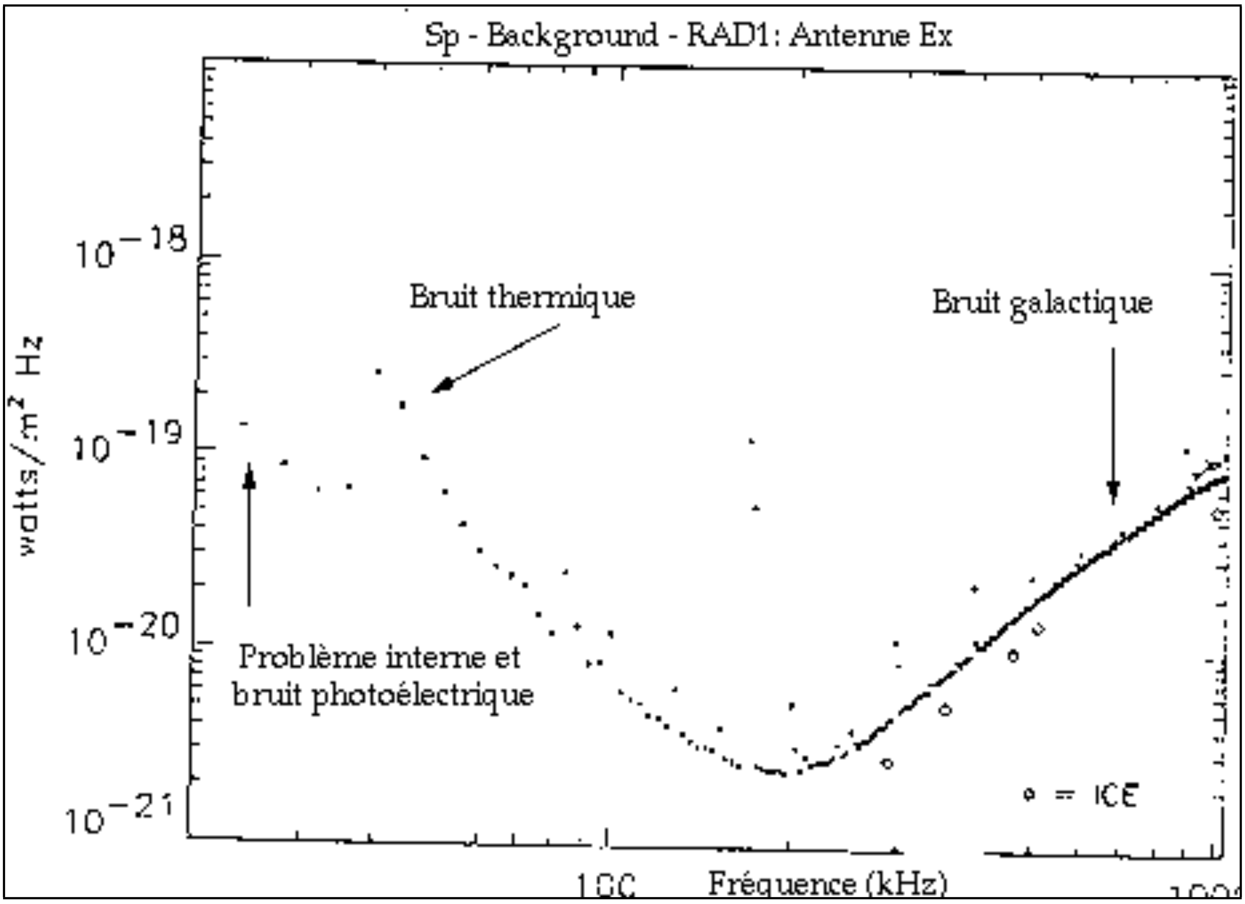
Sp - Background - RAD1: Antenne Ex
watts/m² Hz
Bruit thermique
Bruit galactique
Problème interne et
bruit photoélectrique
∘ = ICE
Fréquence (kHz)

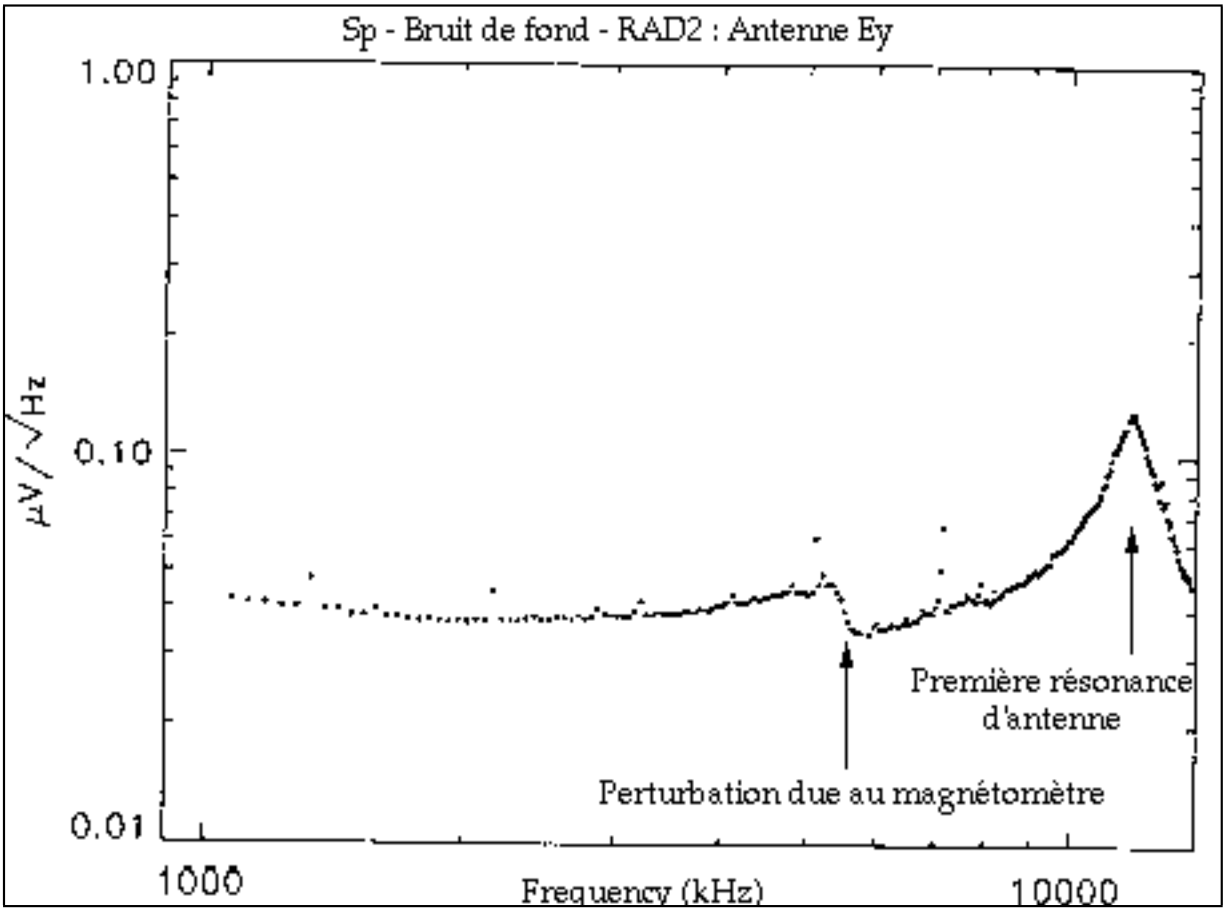
Sp - Bruit de fond - RAD2 : Antenne Ey
1.00
0.10
0.01
μV/√Hz
Première résonance
d'antenne
Perturbation due au magnétomètre
1000
Frequency (kHz)
10000

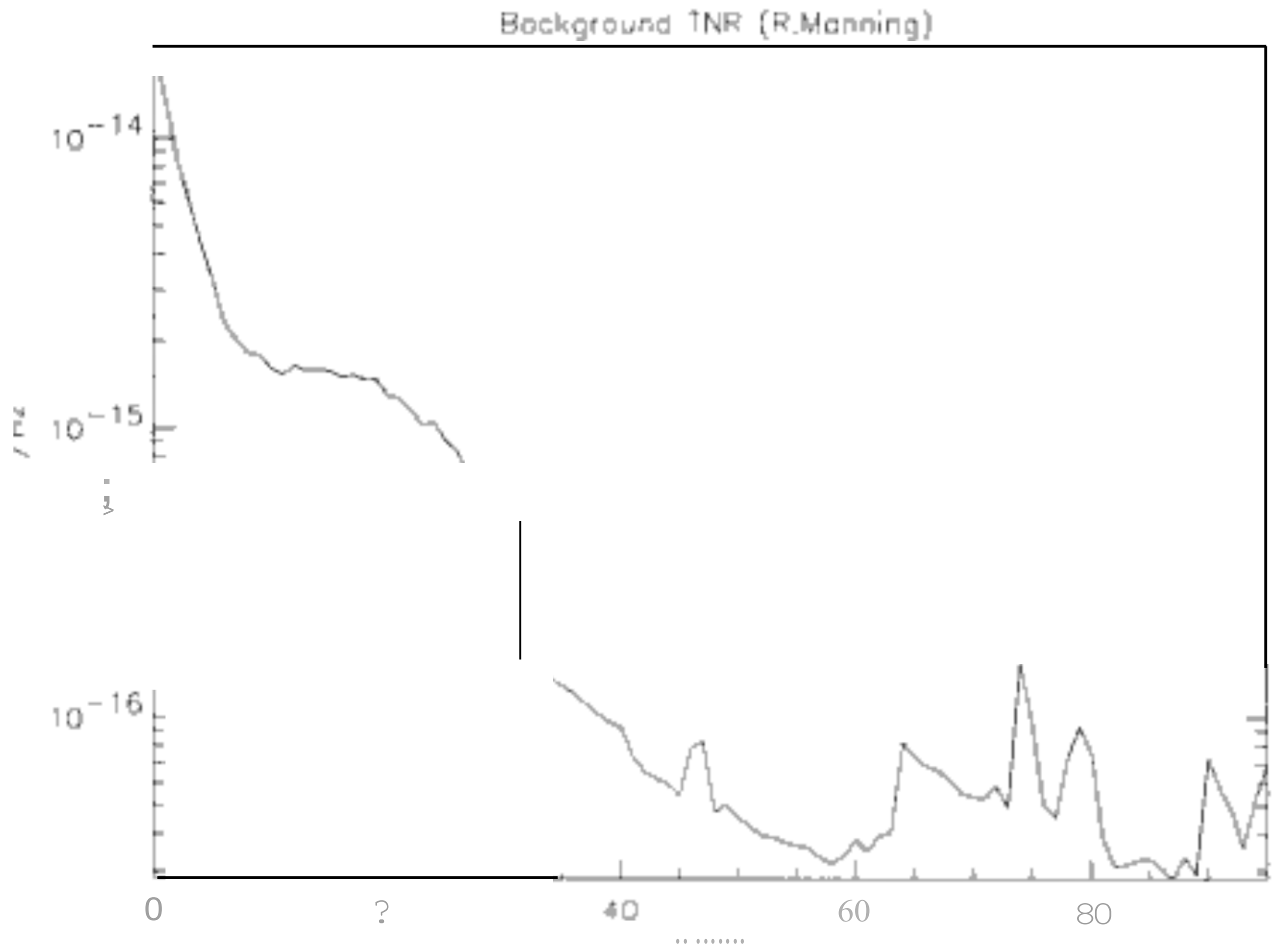
Background TNR (R.Manning)
$10^{-14}$
$10^{-15}$
$10^{-16}$
0
?
40
60
80

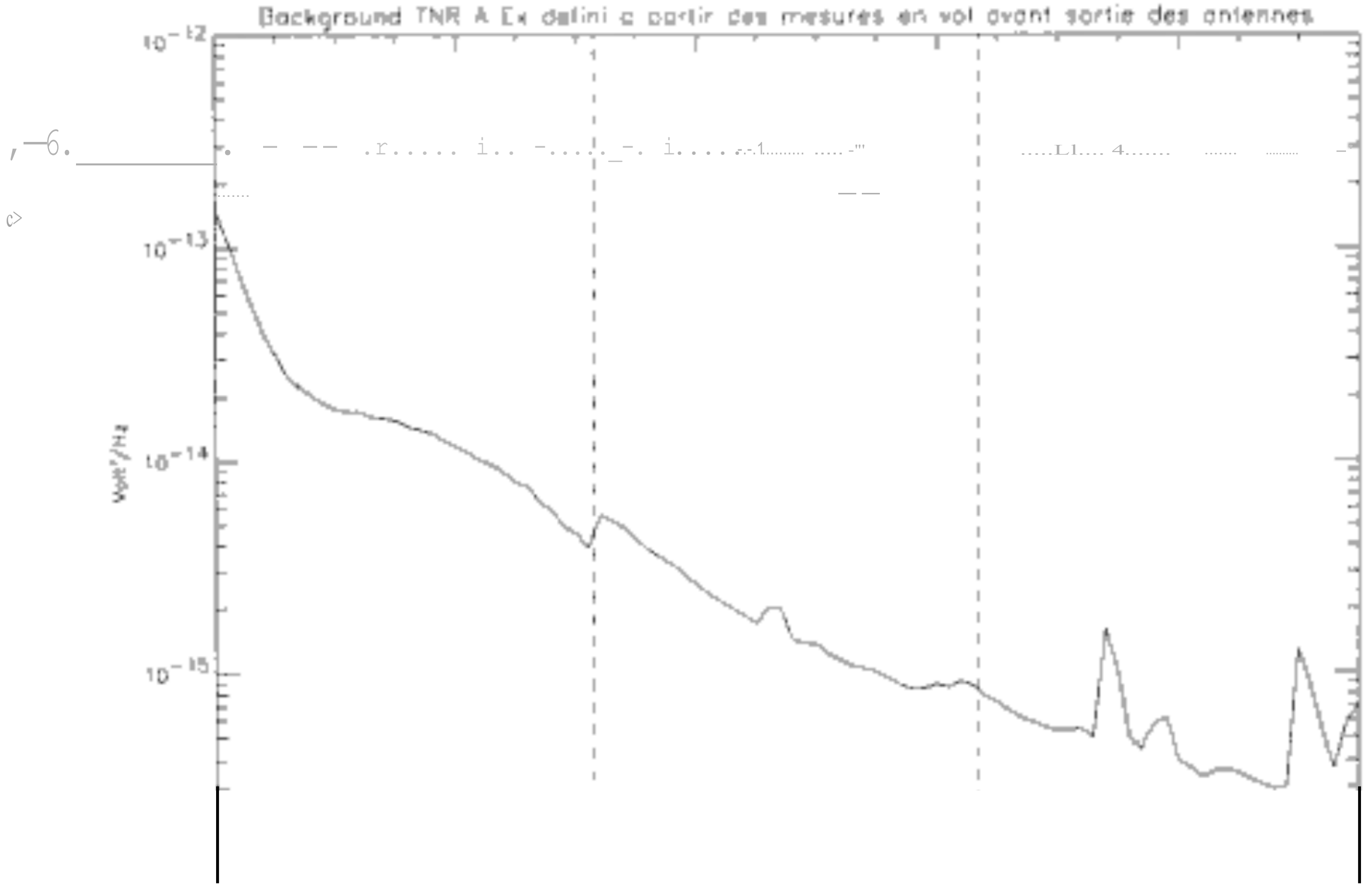
Background TNR A Ex defini a partir des mesures en vol avant sortie des antennes
$10^{-12}$
$10^{-13}$
$10^{-14}$
$10^{-15}$
Volt²/Hz